

AD-A040 380

HARVARD UNIV CAMBRIDGE MASS GORDON MCKAY LAB

F/6 9/5

ARRAYS OF BEVERAGE ANTENNAS.(U)

MAR 77 R M SORBELLO, R W KING, K - LEE

F19628-76-C-0057

UNCLASSIFIED

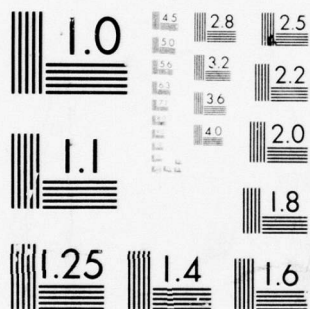
RADC-TR-77-113

NL

| OF |

AD  
A040 380





MICROCOPY RESOLUTION TEST CHART  
NATIONAL BUREAU OF STANDARDS-1963-A

AD A 040380

RADC-TR-77-113  
Final Scientific Report  
March 1977



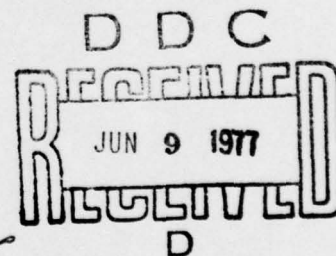
ARRAYS OF BEVERAGE ANTENNAS

by

R. M. Sorbello, R. W. P. King, K.-M. Lee, L. C. Shen and T. T. Wu

Gordon McKay Laboratory, Harvard University  
Division of Engineering and Applied Physics  
Cambridge, MA 02138

Approved for public release;  
distribution unlimited.



AD No. \_\_\_\_\_  
DDC FILE COPY

ROME AIR DEVELOPMENT CENTER  
AIR FORCE SYSTEMS COMMAND  
GRIFFISS AIR FORCE BASE, NEW YORK 13441


This report has been reviewed by the RADC Information Office(01) and is releasable to the National Technical Information Service (NTIS). At NTIS it will be releasable to the General public, including foreign nations.

This technical report has been reviewed and approved for publication.

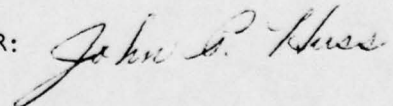
APPROVED:

  
JOHN F. McILVENNA  
Project Engineer

APPROVED:

  
ALLAN C. SCHELL  
Acting Chief  
Electromagnetic Sciences Division

FOR THE COMMANDER:



Plans Office



Unclassified

SECURITY CLASSIFICATION OF THIS PAGE (When Data Entered)

19 REPORT DOCUMENTATION PAGE		READ INSTRUCTIONS BEFORE COMPLETING FORM
1. REPORT NUMBER RADC-TR-77-113	2. GOVT ACCESSION NO.	3. RECIPIENT'S CATALOG NUMBER
4. TITLE (and Subtitle) ARRAYS OF BEVERAGE ANTENNAS	5. TYPE OF REPORT & PERIOD COVERED Final Report: September 24, 1975 - September 30, 1976	
7. AUTHOR(s) R. M. Sorbello, R. W. P. King, K.-M. Lee, L. C. Shen and T. T. Wu	8. CONTRACT OR GRANT NUMBER(s) F19628-76-C-0057 and Joint Services Electronics Program Contract N00014-75-C-0648	
9. PERFORMING ORGANIZATION NAME AND ADDRESS Gordon McKay Laboratory, Harvard University Division of Engineering and Applied Physics Cambridge, MA 02138	10. PROGRAM ELEMENT, PROJECT, TASK AREA & WORK UNIT NUMBERS 61102F 5635-06-01	
11. CONTROLLING OFFICE NAME AND ADDRESS Deputy for Electronic Technology (RADC/ETER) Hanscom AFB, MA 01731 Contract Monitor: John F. McIlvenna	12. REPORT DATE March 1977	
14. MONITORING AGENCY NAME & ADDRESS (if different from Controlling Office)	13. NUMBER OF PAGES 69	
15. SECURITY CLASS. (of this report) UNCLASSIFIED		15a. DECLASSIFICATION/DOWNGRADING SCHEDULE
16. DISTRIBUTION STATEMENT (of this Report)  Approved for public release; distribution unlimited.		
17. DISTRIBUTION STATEMENT (of the abstract entered in Block 20, if different from Report) Final rept. 24 Sep 75 - 3p Sep 76		
18. SUPPLEMENTARY NOTES		
19. KEY WORDS (Continue on reverse side if necessary and identify by block number) Single horizontal-wire antenna over an imperfectly conducting half-space, terminated (Beverage), open-ended (finite) and short-circuited (infinite), circuit and radiating properties generalized theory and experiment (fresh and salt water, moist earth) (CONTINUED ON REVERSE SIDE)		
20. ABSTRACT (Continue on reverse side if necessary and identify by block number) A summary of the research performed under RADC/ETER Contract F19628-76-C- 0057 on Arrays of Beverage Antennas is presented. It begins with a discussion of the theoretical and experimental determination of the circuit and radiating prop- erties of single horizontal-wire antennas over an imperfectly conducting half- space. This study was reported earlier, in detail, in Scientific Reports Nos. 1 (Vols. I and II) and 2. The antennas are either loaded with a resistor and a quarter-wave section of line to form the modified Beverage antenna or are open- (CONTINUED ON REVERSE SIDE)		

DD FORM 1 JAN 73 1473

EDITION OF 1 NOV 65 IS OBSOLETE

UNCLASSIFIED

SECURITY CLASSIFICATION OF THIS PAGE (When Data Entered)

157000

19. Key Words (Continued)

Coupled horizontal-wire antennas over an electrically dense dissipative half-space, terminated (Beverage) and open-ended, circuit properties, symmetrical and antisymmetrical excitations, generalized theory, fresh- and salt-water measurements

20. Abstract (Continued)

ended. King's theory for the unloaded antenna is extended to apply to the terminated Beverage antenna. Measurements made on both types of horizontal antenna when placed at varying heights above fresh water, salt water and moist earth are compared with theory. The results indicate the need to include end effects in the analysis. This topic concludes with a discussion of the semi-empirical method subsequently developed to determine the end effects as represented by a complex terminal function which takes account of radiation into the air and, at the same time, corrects for the capacitive end effect. The usefulness of this method in extending the theory to greater antenna heights is demonstrated in a paper comparing theory and experiment for short-circuited (effectively infinite), open-ended (finite) and terminated (Beverage) antennas over fresh and salt water.

A similar study of the circuit properties of coupled parallel horizontal-wire antennas above an electrically dense dissipative half-space is then reported. The complex wave number, distribution of current and admittance of the antennas are determined theoretically for symmetrical and antisymmetrical excitations. The theory is generalized, as for the single horizontal antenna, to take account of radiation into the air through a complex terminal function and so enlarge its range of validity while preserving the transmission-line form. This function is determined from a least-squares fit of the measured and theoretical current distributions. Current measurements were made on coupled horizontal antennas, driven in zero-phase and first-phase sequences, for six different antenna separations and three different heights above fresh- and salt-water solutions. The antennas were either open-ended or terminated in a lumped resistor and a quarter-wave extension of the antenna to produce traveling-wave distributions of current. Good agreement is displayed between theoretical and measured currents on the open-ended antennas and between theoretical and measured values of the terminal function for the terminated, modified Beverage antennas. The section on the two-element Beverage array concludes with a brief discussion of measurements made on two coupled Beverage antennas in a collinear configuration. Tables of the currents measured on one element of a two-element collinear array of Beverage antennas over fresh- and salt-water solutions when driven symmetrically and antisymmetrically are provided. They are seen to be like those on the same element when isolated.

# EVALUATION

This Final Report summarizes the work on single and two element Beverage antennas. The intent of the effort was to develop and experimentally verify an expression for the current along a single Beverage antenna that would completely characterize the structure over a variety of ground parameters and antenna heights typical of those encountered in OTH radar systems. Measurements on arrays of two Beverage antennas in the parallel and endfire geometries over the heights and ground parameters of the single element case showed that interelement effects are of little concern. A current expression for these arrays was also developed and checked against the measurements. The study provides the basic information on Beverage antennas from which system parameters such as gain, front-to-back ratio etc. can be developed.

*John M. McIlvenna*  
JOHN McILVENNA  
Project Engineer

ACCESSION for	
NTIS	White Section <input checked="" type="checkbox"/>
DDC	Buff Section <input type="checkbox"/>
UNANNOUNCED	<input type="checkbox"/>
JUSTIFICATION.....	
BY.....	
DISTRIBUTION/AVAILABILITY CODES	
Dist.	AVAIL. and/or SPECIAL
A	

DDC  
RECEIVED  
JUN 9 1977  
D

## TABLE OF CONTENTS

	<u>PAGE</u>
I. Introduction. . . . .	1
II. The Single-Wire Beverage Antenna. . . . .	2
A. Circuit Properties . . . . .	2
B. Radiation Field Patterns . . . . .	5
C. Theoretical Refinements. . . . .	7
D. The Horizontal-Wire Antenna Over a Dissipative Half-Space:	
Generalized Formula and Measurements . . . . .	9
1. The Infinitely Long Horizontal-Wire Antenna . . . . .	9
2. Horizontal-Wire Antenna of Finite Length. . . . .	20
3. Description of Experiment . . . . .	25
4. Discussion of Results and Conclusion. . . . .	25
5. References. . . . .	28
III. The Two-Element Beverage Array. . . . .	29
A. Coupled Horizontal-Wire Antennas Over a Conducting or	
Dielectric Half-Space. . . . .	29
1. Introduction. . . . .	30
2. Approximate Solution for the Currents in Coupled	
Insulated Antennas. . . . .	30
3. Two Horizontal Wires Over a Half-Space. . . . .	35
4. Numerical Results . . . . .	39
5. Generalization of the Theory to Greater Antenna Heights . .	39
6. Description of the Experiment . . . . .	43
7. Evaluation of Terminal Functions; Comparison of	
Theory and Experiment . . . . .	46
8. Conclusion. . . . .	52
9. Appendix. . . . .	53
10. References. . . . .	54
B. Measured Currents on Two Coupled Collinear Beverage	
Antennas . . . . .	55
IV. Publications. . . . .	63



## I. Introduction

The originally developed theory of the horizontal-wire antenna involved the implicit assumption that radiation into the air is negligible compared with the power transfer into the imperfectly conducting or dielectric half-space (earth). This is a good approximation when the antenna is quite close to the earth ( $d/\lambda_0 \leq 0.02$ ). In order to generalize the theory to higher antennas, account must be taken of radiation into the air. Since this changes the current from the simple transmission-line form to the much more complicated distribution characteristic of an isolated antenna as the height is increased, a rigorous solution of the problem is difficult. Fortunately, the transmission-line form is a reasonable approximation for heights up to at least a quarter wavelength and the effect of radiation into the air can be treated approximately as a property of the open end in the shape of a lumped terminating impedance. This generalization and its experimental verification is described in Section II.

A theory of coupled parallel horizontal-wire antennas is derived and confirmed experimentally in Section III. The theory is approximate in the same sense as the earlier theory of the single horizontal-wire antenna in that radiation into the air is neglected and a limitation to small heights is imposed. This restriction is then modified by the introduction of suitably defined terminal impedances to take account of radiation into the air as an end effect. The numerical values of the terminal functions are determined from comparisons of measured and theoretical current distributions. Section III concludes with a brief description of measurements made on two coupled collinear Beverage antennas placed over fresh- and salt-water solutions. The results show that the coupling between the elements is generally negligible.

Finally, in Section IV a list has been prepared of the Scientific Reports, published papers and papers presented at Scientific Meetings that have been supported by RADC/ETER Contract F19628-76-C-0057.

## II. The Single-Wire Beverage Antenna

### A. Circuit Properties

The results of a theoretical and experimental study of the circuit properties of single-wire antennas placed horizontally above an imperfectly conducting half-space have been reported ["The Beverage Wave Antenna: Currents, Charges and Admittances. I. Theoretical Analysis; Experimental Equipment and System Calibration. II. Experimental Measurements," Scientific Report No. 1 (Vols. I and II), RADC/ETER Contract F19628-76-C-0057, by R. M. Sorbello]. This investigation gave particular emphasis to the Beverage wave antenna, a special type of horizontal-wire antenna placed in close proximity to the earth and resistively terminated at each end. Earlier work has generally assumed a free-space wave number on the wire, thus neglecting the effect of the half-space. The present study has carefully investigated experimentally the effect of the half-space on the circuit properties (current, charge and input admittance) of the antenna and has included this effect in all theories discussed. A brief summary of the theoretical developments and experimental results contained in Scientific Report No. 1 follows.

To begin with, the conventional design of the Beverage wave antenna was modified in Section 1.5 to eliminate the many difficulties encountered when the proper ground conditions cannot be achieved. It was necessary to devise a driving method which would avoid making physical contact with the ground. This was accomplished by loading the wire both with a resistor and a quarter-wavelength-long section of transmission line. The proper resistor is chosen to obtain a matched condition on the line. The quarter-wavelength section transforms back to the resistor as a high reactance or short circuit and represents a pseudo-ground connection at that point. This design avoids the problems of the original grounding system and possesses all the desired properties of the conventional Beverage antenna.

The modified Beverage antenna was then analyzed in Section 1.6 by simply extending the theory of King, Wu and Shen, summarized in Section 1.2, for the unloaded horizontal wire over an interface to cover the case of loaded wires as well. Standard transmission-line techniques were employed to obtain the current distribution on an asymmetrically driven, doubly loaded horizontal-wire antenna over a dissipative medium for the general case with any combina-



tion of lengths and values of loads. The special cases of symmetrically and asymmetrically driven, modified Beverage antennas with  $Z_1 = Z_2 = Z_c$  and  $\ell_2 = \ell_4 = \lambda_L/4$  are then treated in Section 1.7.

The construction and operation of the experimental equipment are dealt with in Part II of Scientific Report No. 1 (Vol. I). It begins with a section on the scale modeling of the electrical properties of a dissipative medium. The criteria involved in selecting an operating frequency of 300 MHz are then discussed in Section 2.2. These include 1) keeping the electrical radius of the wire a small fraction of a wavelength, 2) allowing the length of the antenna to vary by several wavelengths, 3) assuring the dimensions of the tank will approximate an infinite half-space, 4) and keeping the smallest antenna height above the half-space, e.g.,  $.01\lambda_0$ , large enough to maintain constant spacing over the length of the wire. Separate apparatus for measurements over water and over earth are described. The different equipment and techniques used to measure the electrical properties of water and of earth are presented in Sections 2.5 and 2.6, respectively. Error estimates are given of the effects of the finite size of the tank and the accuracy of the measuring probes. Finally, the methods of calibrating the impedance, current and charge measurements are discussed in Section 2.8.

The measured distributions of current and charge and measured input admittances are presented in extensive graphs and tables in Part III of Scientific Report No. 1 (Vol. II). Current and charge measurements were made on unloaded horizontal-wire antennas and on modified Beverage wave antennas of length  $h/\lambda_0 = .5, 1.0$  and  $1.5$  at heights of  $d/\lambda_0 = .01, .02, .05, .1$  and  $.25$  above three different media - fresh water ( $\epsilon_r = 82, \sigma = .092$  mho/m), salt water ( $\epsilon_r = 81, \sigma = 3.9$  mhos/m) and moist earth ( $\epsilon_r = 11.4, \sigma = .0022$  mho/m). The closest height for all moist-earth measurements was  $d/\lambda_0 = .02$ . Admittance measurements for the horizontal-wire antennas were made for lengths ranging from  $h/\lambda_0 = .013$  to  $1.5$ . Only four lengths,  $\ell_1/\lambda_0 = .25, .5, 1.0$  and  $1.5$ , were used when taking admittance measurements on the modified Beverage antennas since the input admittance remains practically constant for increasing antenna lengths.

The measured data were normalized in most cases to the accompanying theoretical curve at  $z/h = .2$  or to a smooth part of the curve in the immediate vicinity of this point. Discrepancies between the experimental results

and the zeroth-order theory of King, Wu and Shen were observed in a large number of cases. For the moist-earth measurements (where the agreement was poorest), these variations could be attributed in part to the violation of condition (1.3b), viz.,  $|k_2| \gg |k_1|$ . For the fresh- and salt-water measurements, the fact that the discrepancies became more pronounced as  $d/\lambda_0$  was increased above .02 led to the conclusion that the spacing was too great to sustain the transmission-line-like form of current predicted by the zeroth-order theory and that, instead, the antenna behavior was approaching that of an antenna in free space. End effects were also believed to account for some of the disagreement found with all three media. (This initial assessment was later changed and end effects were shown to be the major source of the disagreement. The final theoretical formulation which includes end effects is described later under Subheading C.). A semi-empirical approach was developed to overcome the significant deviations existing between experimental and theoretical results. The zeroth-order formulas for the current, charge and admittance were used with the theoretically predicted wave number replaced by a measured effective value, defined as the wave number observed on the unloaded dipole antenna. This approach produced good agreement with the experimental data for the distributions of current and charge, poorer agreement for the admittance.

In Part III (Vol. II) of Scientific Report No. 1 the experimental data are compared with the King, Wu and Shen theory for small values of  $d/\lambda_0$  ( $= .01$  and  $.02$ ) - i.e., where these agree well - and with both the semi-empirical approach and the theory for the larger values of  $d/\lambda_0$  - where theory and experiment no longer correspond. For fresh- and salt-water measurements on unloaded horizontal antennas, noticeable disagreement between theory and experiment first appears at  $d/\lambda_0 = .05$  and  $.1$  and is mainly confined to the attenuation  $\alpha_L$ . The agreement between the semi-empirical approach and experiment for  $d/\lambda_0 = .05$  and  $.1$  is good except for the admittance near first resonance. The semi-empirical approach provides only an approximate representation of the current and charge for  $d/\lambda_0 = .25$ , and even poorer agreement for the admittance. A look at the results for modified Beverage wave antennas over fresh or salt water shows overall better agreement between experiment and both the purely theoretical values (fairly good up to  $d/\lambda_0 = .1$ ) and those obtained using the measured effective wave numbers (good agreement even for  $d/\lambda_0 = .25$  except for the admittance).

King's theory does not compare well with experimental data for any of the antenna heights studied when moist earth is the dissipative medium because  $|k_2| \gg |k_1|$  is not strictly true and also because of end effects. The semi-empirical approach also shows poorer agreement for the moist-earth measurements than for those over fresh or salt water. It gives satisfactory agreement for the current and charge distributions on unloaded horizontal wires at heights up to  $d/\lambda_0 = .1$ , while the admittance is poor at  $d/\lambda_0 = .1$  especially in the second and third resonances. On the other hand, the semi-empirical approach does agree well with experiment for the distributions of current and charge on modified Beverage antennas at heights up to and including  $d/\lambda_0 = .25$  over moist earth. The admittance of these modified Beverage antennas shows variations in the susceptance at all heights greater than  $d/\lambda_0 = .02$ . It is interesting to note that, although  $|k_2| > |k_1|$  for moist earth at 300 MHz, at much lower frequencies for which  $p_e = \sigma/\omega\epsilon$  becomes increasingly larger and the earth acts more like a conductor, the condition  $|k_2| \gg |k_1|$  can be obtained for moist earth. Under these conditions, one can expect that King's theory will hold in a manner analogous to the water cases.

#### B. Radiation Field Patterns

The results of a theoretical and experimental investigation of the transmitting and receiving properties (far-field radiation patterns) of horizontal-wire antennas placed over an imperfectly conducting half-space have been reported ["The Beverage Wave Antenna: Radiation Field Patterns," Scientific Report No. 2, RADC/ETER Contract F19628-76-C-0057, by R. M. Sorbello]. Particular attention is given in this report to the Beverage wave antenna. Early work by Sommerfeld showed that the radiation from a dipole above an imperfect earth could be separated into a space wave (which could reflect off the ionosphere and which predominates at large distances above the earth) and a surface wave (which could diffract around the curvature of the earth and which dominates close to the surface). Because of the difficulties involved in solving the Sommerfeld integral formulation, asymptotic approximations valid in the radiation zone have generally been employed to solve this problem. The useful approximate forms developed earlier by Norton have been used in this study, the only difference being that in the present analysis the exact expressions for the antenna current are used rather than an assumed current distribution. An expression for the space-wave radiation pattern is

formulated using a "geometric optics" approximation, while the superposition principle is used to sum the fields of individual infinitesimal dipoles to obtain the surface-wave radiation pattern. Expressions for a number of useful antenna parameters (efficiency, front-to-back ratio, antenna gain, and effective length) are then derived.

A series of experimental measurements were made both to verify the accuracy of the approximate theoretical formulation and to verify that the asymmetrically driven, modified Beverage antenna can be used to obtain unidirectional surface-wave and space-wave radiation patterns that are equivalent to those of the conventional Beverage antenna. Measurements were made of the vertical component of the surface wave (the major field component in the radiation zone) of modified Beverage antennas,  $1.0\lambda_0$  in length, placed at heights ranging from  $d/\lambda_0 = .01$  to  $d/\lambda_0 = .25$  over fresh water ( $\epsilon_r = 81$ ,  $\sigma = .062$  mho/m) and dry earth ( $\epsilon_r = 4.3$ ,  $\sigma = .0013$  mho/m). The operating frequency of 144.06 MHz used in the experimental model corresponds by a scale factor of 5 to a full-scale frequency of 30 MHz. Descriptions are given of the experimental apparatus including the special polyfoam support structure and balun required in order to drive asymmetrically the modified Beverage antenna over both earth and water.

The ability of the modified Beverage antenna to launch a unidirectional surface-wave radiation pattern is clearly evident. In use over both fresh water and dry earth, front-to-back ratios of 20 dB can be obtained. The main radiation lobe is quite broad with half-power beamwidths of about  $80^\circ$ . Although no measurements were made to confirm this fact, unidirectional characteristics should also be exhibited in the space-wave radiation pattern. The conclusion is reached that modified Beverage antennas should be excellent elements in highly directive broadside arrays. Measurements made to determine the effect of the antenna spacing and the properties of the half-space on the radiation patterns indicate 1) that when properly matched the vertical surface-wave pattern appears to be fairly insensitive to changes in height in the  $.01 \leq d/\lambda_0 \leq .1$  range and 2) that for  $d/\lambda_0 = .25$  a significant loss in directivity is noticed along with changes in the shape of the pattern at  $\phi = 0^\circ$ . These seem to be attributable to the changing nature of the antenna current distribution from one that is predominantly transmission-line-like to one more characteristic of an antenna in free space.



### C. Theoretical Refinements

As indicated earlier in the discussion of the circuit properties, the use of a measured effective wave number did not provide as satisfactory or complete an explanation of the discrepancies between the measured and purely theoretical results as had been hoped. A number of theoretical and experimental investigations were performed consequently to resolve this problem. These are described in Section 1.8 of Scientific Report No. 1 (Vol. I). A summary of the major developments follows.

A closer examination of the problem by Professor T. T. Wu led to the postulate that as long as  $h/d$  remains large, the transmission-line form of the current will be valid and the theoretical expression (1.7) will give the correct wave number. If true, this would replace the more restrictive condition on  $d$  given in (1.3c) and would suggest that the observed discrepancies are not due to  $d/\lambda_0$  being too large. An experimental procedure was developed to verify this postulate. In order to eliminate all influence of end effects, the decision was made to use short-circuit terminations since the imaging effect of the short circuit, whereby the antenna appears to be doubled in length, provides a termination with almost ideal characteristics. With open-ended antennas this could be accomplished only if the wire were infinitely long. The measurements were made on terminated antennas,  $1.5\lambda_0$  in length, placed over a fresh-water solution ( $\epsilon_r = 82$ ,  $\sigma = .092$  mho/m). The short-circuit termination was made out of a large 4' by 4' aluminum sheet. The cumulative effect of the two image planes, the one against which the antenna is driven and the terminating plane, is to create a successive series of images that gives the appearance of an infinitely long antenna. If Wu's postulate is correct, the measured wave numbers should agree with the theoretical results obtained from (1.7). The agreement is found to be excellent with less than a 5% error occurring for spacings up to  $d/\lambda_0 = .25$ . Additional measurements made on finite antennas indicate that for values of  $h/d \gtrsim 10$  it is possible to use King's theory and have (1.7) give the correct wave number.

It follows from these measurements that end effects are indeed the primary cause of the disagreement originally found between the theoretical and experimental values of current, charge and admittance for loaded and unloaded horizontal-wire antennas over an imperfectly conducting half-space. In fact,

it can be shown that these end effects are related to the actual radiating mechanism of the antenna. In King's original theory the wave number for the antenna was derived with the assumption that radiation into the air is negligible compared to radiation into the dissipative medium. When  $d/\lambda_0$  becomes sufficiently large and the influence of the half-space begins to diminish, the antenna can begin to radiate a significant amount of energy into the air. This added loss can be observed in the measured effective  $\alpha_L$  which is larger than that predicted by theory for  $d/\lambda_0 \geq .05$ . Because an analytical solution promised to be too complex, the following experimental approach was developed.

For  $d/\lambda_0$  not too great, the loss associated with radiation into the air can be accounted for by a complex terminating impedance  $Z_s$ , the real part of which is the resistance associated with radiation into the air while the imaginary part is the reactance associated with the capacitive end effect at the open end. The original theoretical formulas for the current, charge and admittance were modified to include the complex terminal function  $\theta_s = \rho_s - i\phi_s = \coth^{-1}(Z_s/Z_c)$ . A computer program to determine  $\theta_s$  from a least-squares fit of the measured and theoretical current distributions was then developed. With the  $\rho_s$  and  $\phi_s$  values determined numerically from the measured data, the new semi-empirical theory was compared to several cases of previously measured data for all three media. In all cases only the theoretical values for  $k_L$  given by (1.7) were used. For the fresh- and salt-water measurements the agreement is very good. At the driving-point there is some variation which tends to increase with  $d/\lambda_0$ . This is to be expected since the semi-empirical theory does not include any corrections for junction effects. Disagreement also occurs in the admittance curves when  $d/\lambda_0 = .25$ ; it appears that at this height a higher-order theory is necessary for the admittance. Finally, for the moist-earth measurements a correction term to (1.7) remains to be developed which would provide theoretical wave numbers in agreement with measurements. Once an accurate analytic expression for the wave numbers is known, the new semi-empirical theory should be applicable for  $.02 \leq d/\lambda_0 \leq .25$  even when condition (1.3b) is not strictly satisfied.

The usefulness of the terminal function in extending the theory to greater antenna heights is demonstrated in the following paper which compares theory and experiment for short-circuited (effectively infinite), open-ended (finite) and terminated (Beverage) antennas over fresh and salt water.



D. The Horizontal-Wire Antenna Over a Dissipative Half-Space:  
Generalized Formula and Measurements

It is shown and verified by experiment that a horizontal resonant or traveling-wave antenna placed in air close to a dense half-space with the properties of lake or sea water or earth behaves like a terminated lossy transmission line. The terminal impedance is related to the radiation of the antenna into the air and the complex wave number and characteristic impedance are those of an infinitely long line. The complex wave number takes account of both dissipation in and radiation into the dense half-space.

\*\*\*

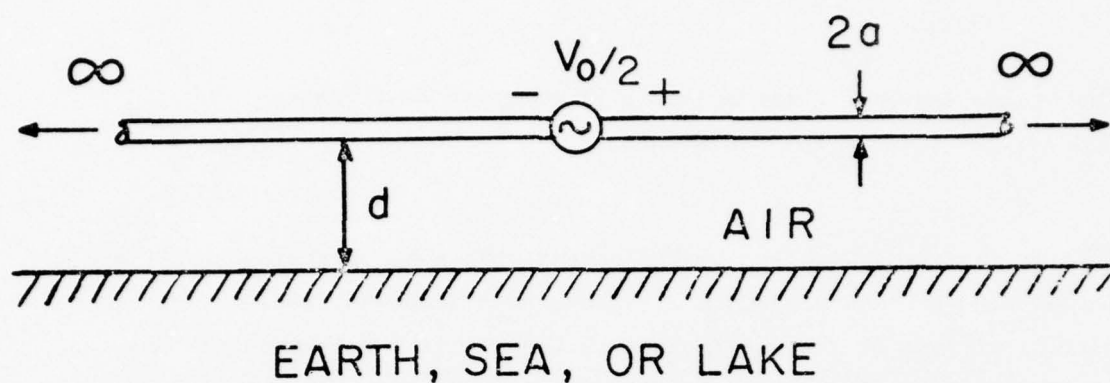
1. The Infinitely Long Horizontal-Wire Antenna

It has been shown [1] that the infinitely long horizontal-wire antenna sketched in Fig. 1(a) behaves mathematically like the transmission line in Fig. 1(b) when, as indicated, it is placed in air close to a dense half-space like a lake, the sea, or the surface of the earth where this is moist. The equivalent transmission line is characterized by a complex wave number  $k_L = \beta_L - j\alpha_L$  and a complex characteristic impedance  $Z_c$ . Simple formulas for  $k_L$  and  $Z_c$  are given in [1, eqs. (28) and (30)] subject to the condition

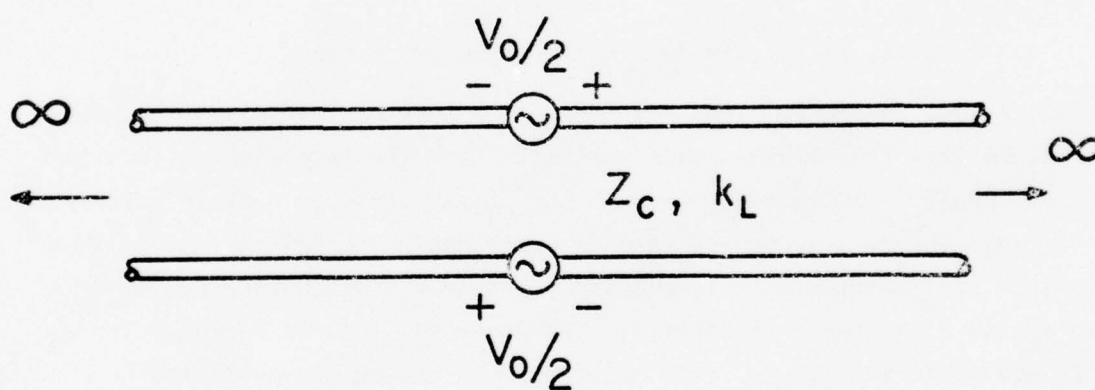
$$|k_4^2| \gg |k_2^2| \quad (1)$$

where  $k_4$  is the complex wave number of the dense half-space and  $k_2 = \beta_0 = \omega/c$  is the real wave number of air. A more general but also considerably more involved formula for  $k_L$  which is valid when  $|k_4^2/k_2^2| \geq 4$  is given in [2, eq. (10)]. When (1) is satisfied, radiation into the air is negligible and the attenuation constant  $\alpha_L$  takes account of both dissipation in and radiation into the lower half-space.

An infinitely long horizontal-wire antenna can be approximated in practice by an antenna of finite length between two sufficiently large vertical



(a)



(b)

FIG. 1 (a) INFINITELY LONG HORIZONTAL-WIRE ANTENNA PLACED IN AIR OVER A DENSE HALF-SPACE. (b) MATHEMATICALLY EQUIVALENT, INFINITELY LONG LOSSY TRANSMISSION LINE.

ground planes as shown in Figs. 2(a) and 2(b) for two methods of driving. With the images in the ground planes these structures correspond to infinitely long, multiply driven and multiply loaded antennas. In Fig. 3 are shown in solid lines the theoretical phase constant  $\beta_L$  and attenuation constant  $\alpha_L$  for the current on the horizontal monopole shown in Fig. 2(b) at a height  $d$  over water with relative permittivity  $\epsilon_r = 82$  and conductivity  $\sigma = 0.092$  Si/m at  $f = 300$  MHz. With  $Z_s = 0$  in Fig. 2(b) the monopole was terminated in a nearly perfect short circuit. The corresponding measured values obtained as described in Section III are shown in Fig. 3 by small circles. The agreement is seen to be excellent over the range  $0 \leq d/\lambda_0 \leq 0.15$ . Measurements were also made at  $d/\lambda_0 = 0.25$  where the theoretical values are  $\beta_L/\beta_0 = 1.000$ ,  $\alpha_L/\beta_0 = 0.0060$ ; the corresponding measured values are  $\beta_L/\beta_0 = 1.004$ ,  $\alpha_L/\beta_0 = 0.0059$  with  $k_2 = \beta_0 = 2\pi \text{ m}^{-1}$ . It is seen that for horizontal-wire antennas terminated in short circuits at both ends (ground planes perpendicular to the wire and the dissipative half-space) the transmission-line form given in [1] yields excellent results for  $k_L = \beta_L - j\alpha_L$  at least when  $0 \leq d/\lambda_0 \leq 0.25$ .

The formula for the current at a distance  $z$  from the base of a monopole with a short-circuited end is

$$I(z) = -jV_0 \cos[k_L(h - |z|)]/Z_c \sin(k_L h) \quad (2)$$

(For the dipole shown in Fig. 2(a) but with  $Z_s = 0$  the same formula applies with an added factor 2 in the denominator.) Theoretical graphs of the current  $I(z)$  given by (2) and the charge per unit length  $q(z)$  obtained from (2) with the equation of continuity,  $\partial I(z)/\partial z + j\omega q(z) = 0$ , are shown in Figs. 4a to 4f for  $d/\lambda_0$  in the range from 0.01 to 0.25;  $\lambda_2 = \lambda_0 = 2\pi/\beta_0$  is the wavelength in air. The length of the monopole between the vertical ground planes is  $h = 1.5\lambda_0$ . The measured points in the distributions of both current and charge per unit length are in excellent agreement with the theoretical curves over the entire range  $0.01 \leq d/\lambda_0 \leq 0.25$ . These graphs in conjunction with the attenuation and phase constants in Fig. 3 provide basic information for understanding the operation of the short-circuited horizontal-wire antenna over a general medium - in this case, water with  $\epsilon_r = 82$  and a conductivity  $\sigma = 0.092$  Si/m which is only slightly above that of lake water. At  $f = 300$  MHz the loss tangent  $p = \sigma/\omega\epsilon = 0.067$  indicates that the water behaves like a very good dielectric.

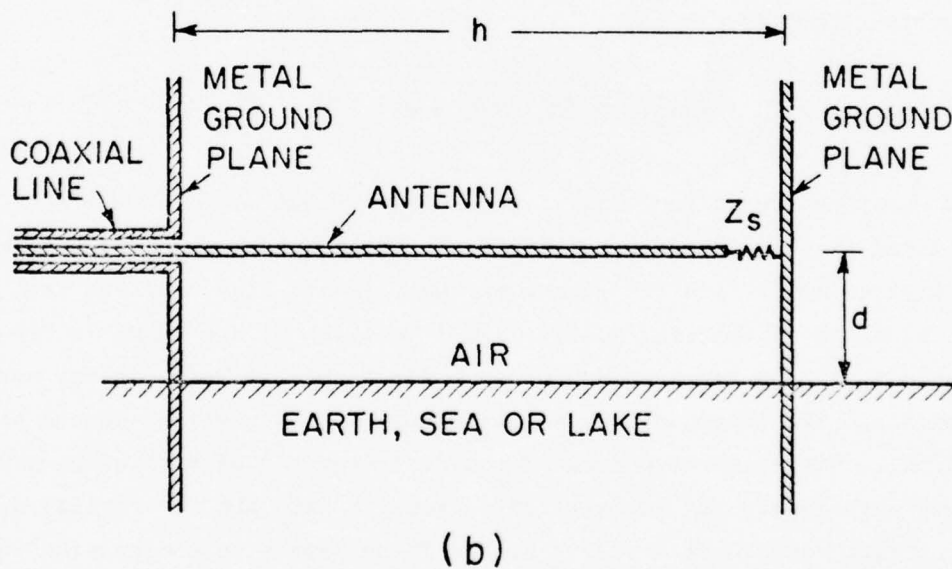
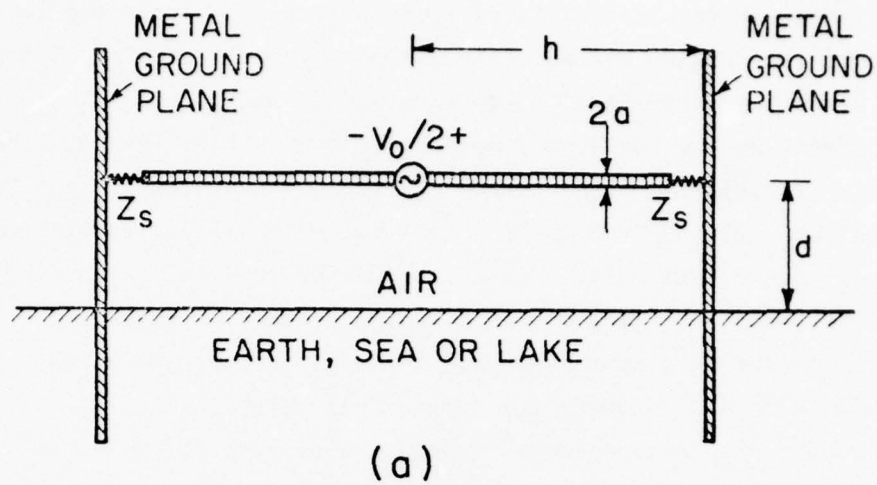


FIG. 2 HORIZONTAL-WIRE ANTENNA OVER A DENSE MEDIUM WHEN TERMINATED AT BOTH ENDS IN A PERFECT SHORT CIRCUIT FOR TWO METHODS OF DRIVING.

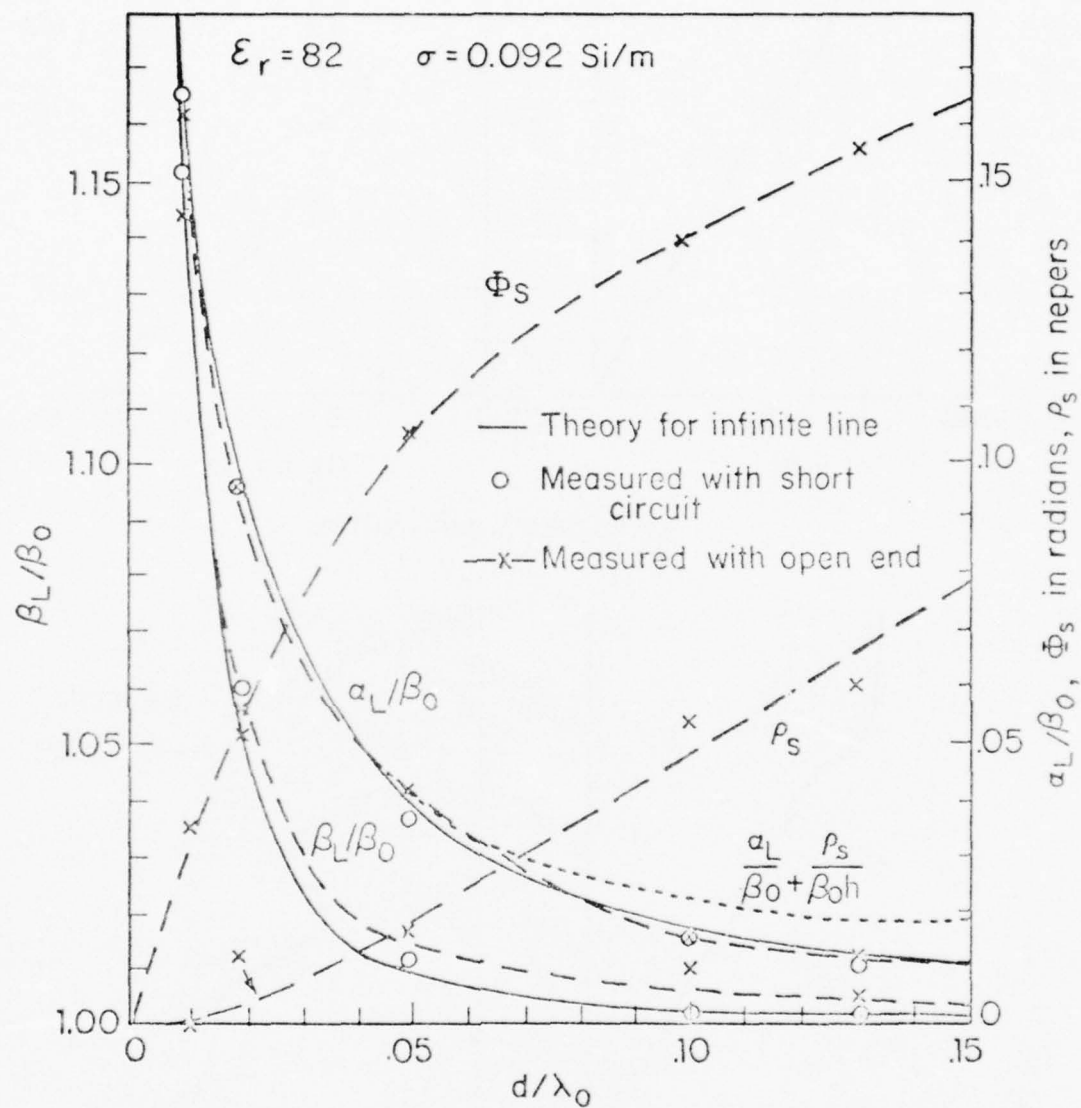
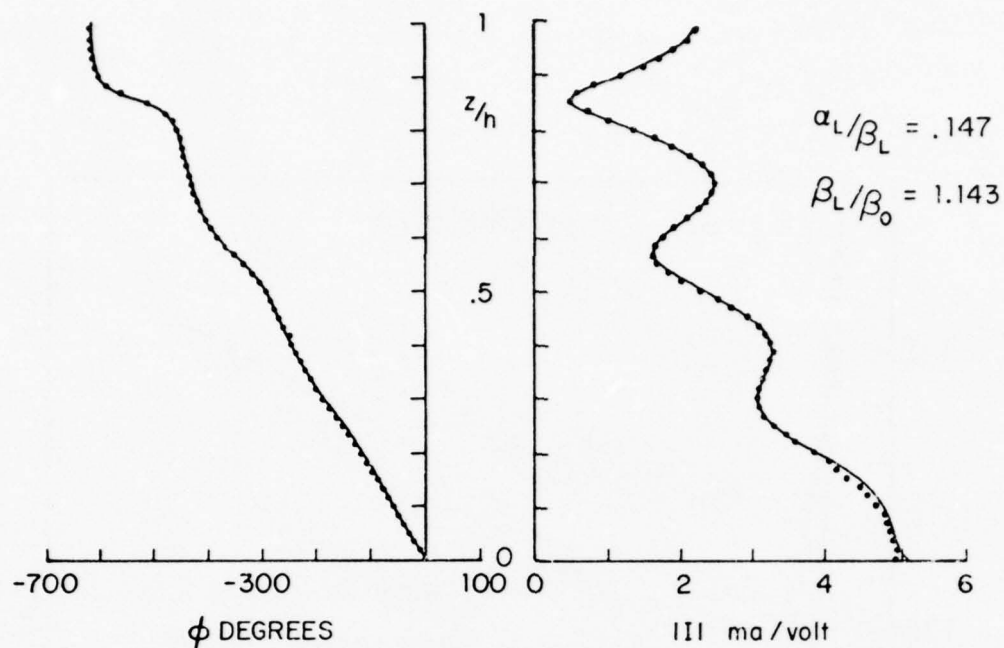
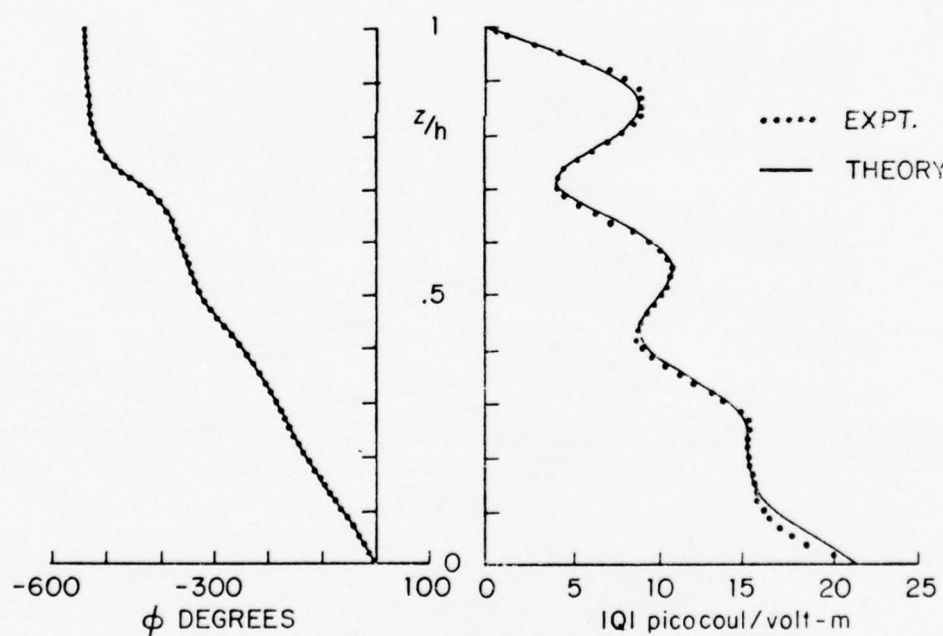


FIG. 3 PHASE AND ATTENUATION CONSTANTS, TERMINAL PHASE AND ATTENUATION FUNCTIONS FOR SHORT AND OPEN-CIRCUITED HORIZONTAL MONOPOLE OVER FRESH WATER.  
 $a/\lambda_0 = 0.0015$ .





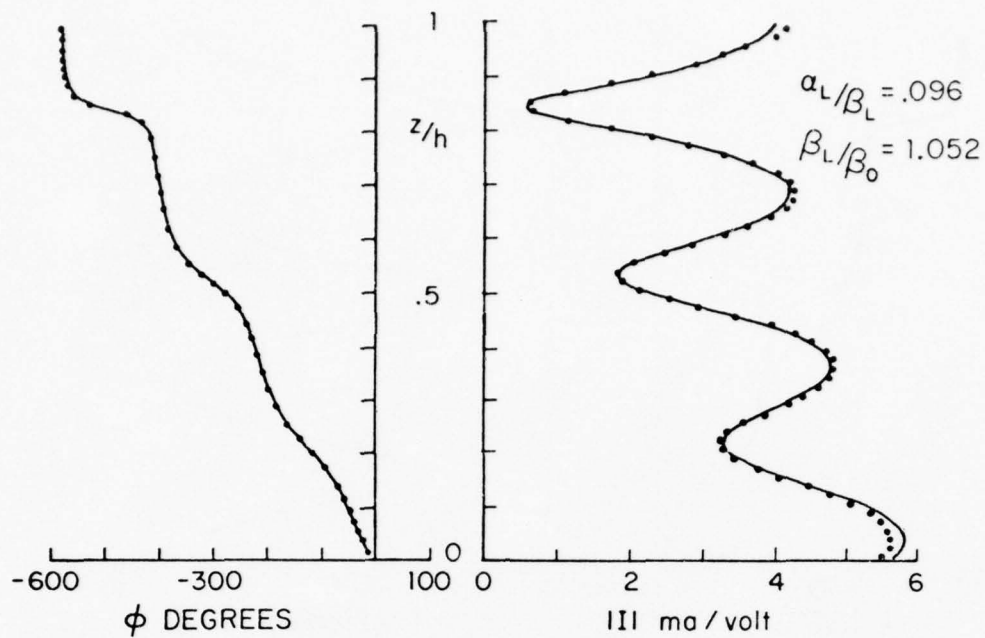
a.) CURRENT DISTRIBUTION



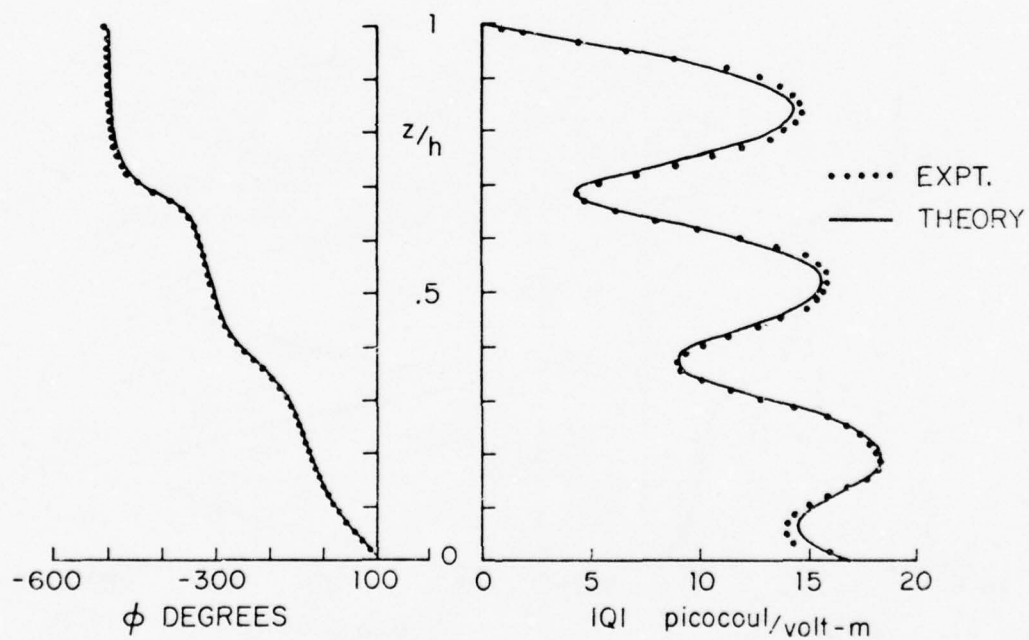
b.) CHARGE DISTRIBUTION

FIG. 4a. CURRENT AND CHARGE DISTRIBUTION ON SHORT-CIRCUITED MONOPOLE OVER FRESH WATER;  $h/\lambda_0 = 1.5$  AND  $d/\lambda_0 = .01$ .  $a/\lambda_0 = 0.0015$ .



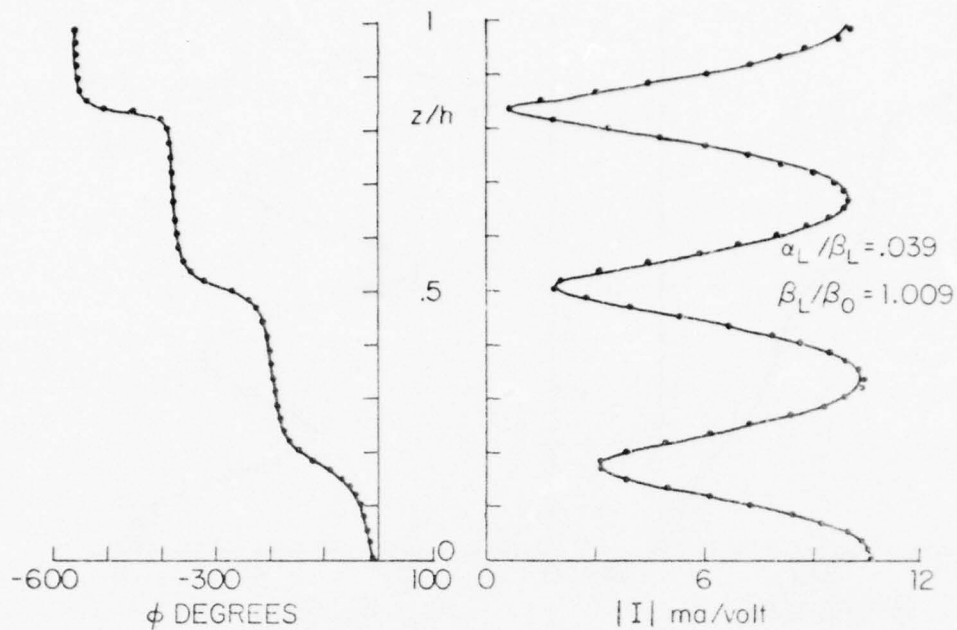


a.) CURRENT DISTRIBUTION

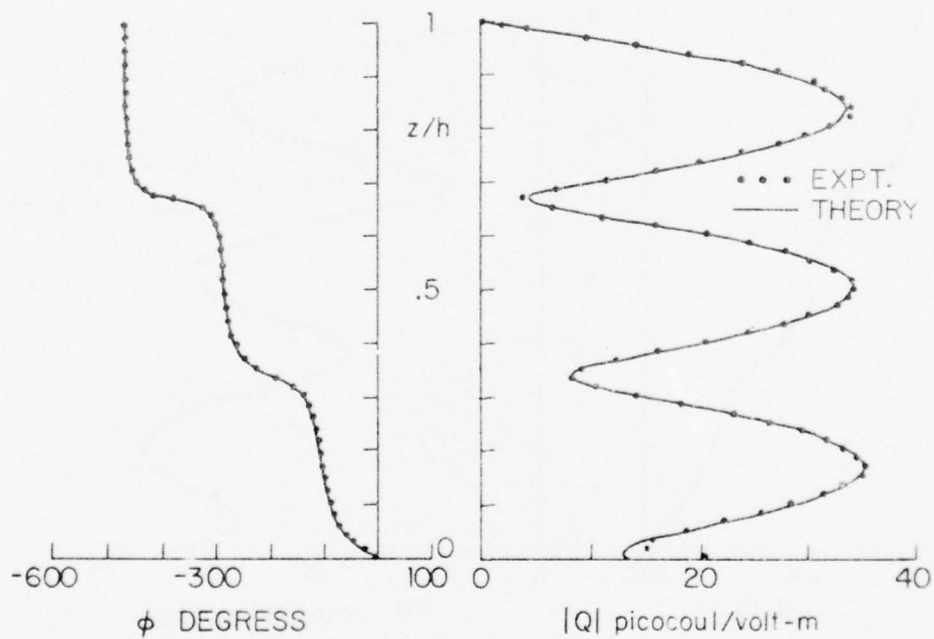


b.) CHARGE DISTRIBUTION

FIG. 4b. CURRENT AND CHARGE DISTRIBUTION ON SHORT-CIRCUITED MONOPOLE OVER FRESH WATER;  $h/\lambda_0 = 1.5$  AND  $d/\lambda_0 = .02$ .  
 $a/\lambda_0 = 0.0015$ .

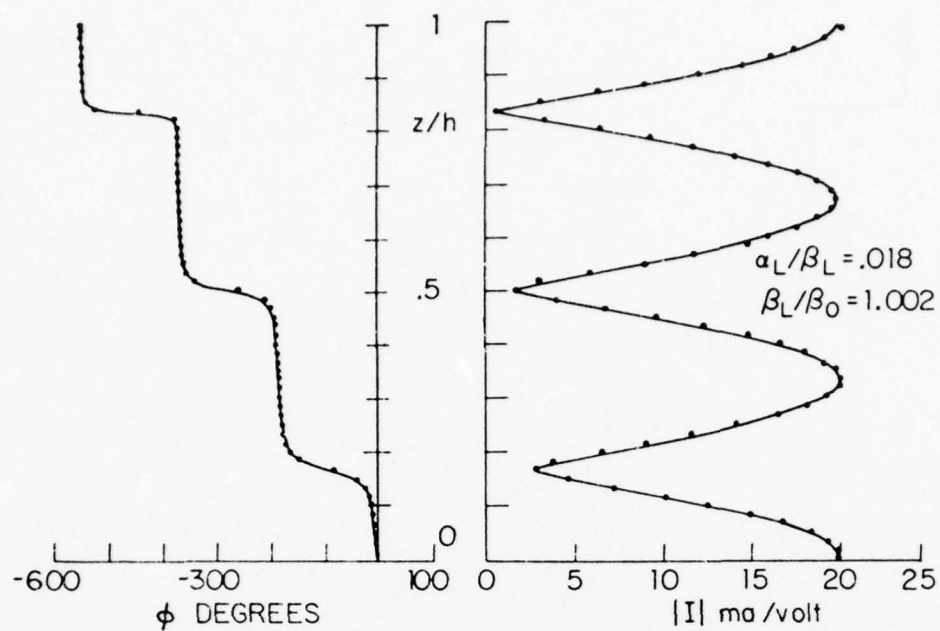


a) CURRENT DISTRIBUTION

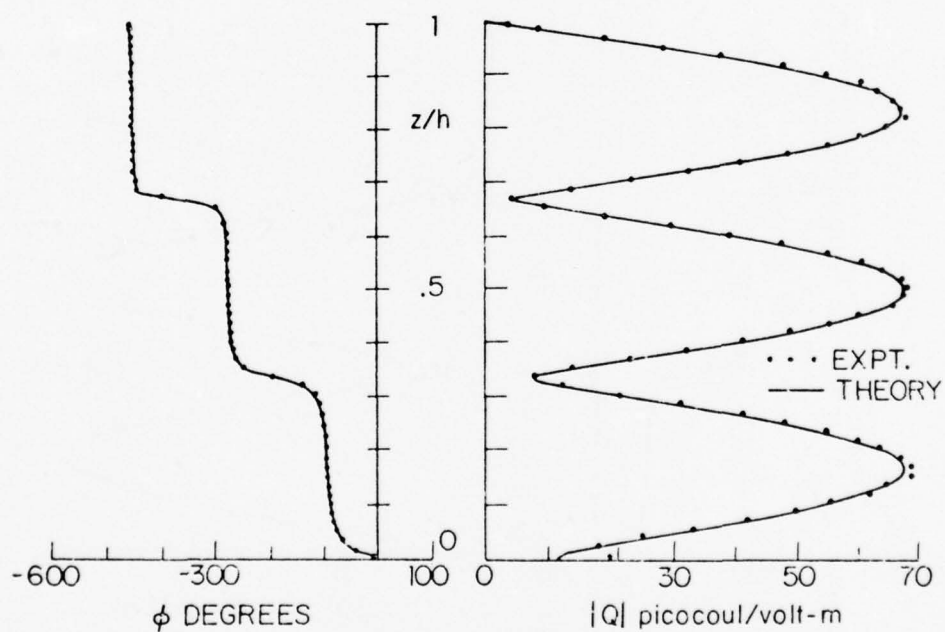


b) CHARGE DISTRIBUTION

FIG. 4c. CURRENT AND CHARGE DISTRIBUTION ON SHORT-CIRCUITED MONOPOLE OVER FRESH WATER;  $h/\lambda_0 = 1.5$  AND  $d/\lambda_0 = .05$ .  
 $a/\lambda_0 = 0.0015$ .

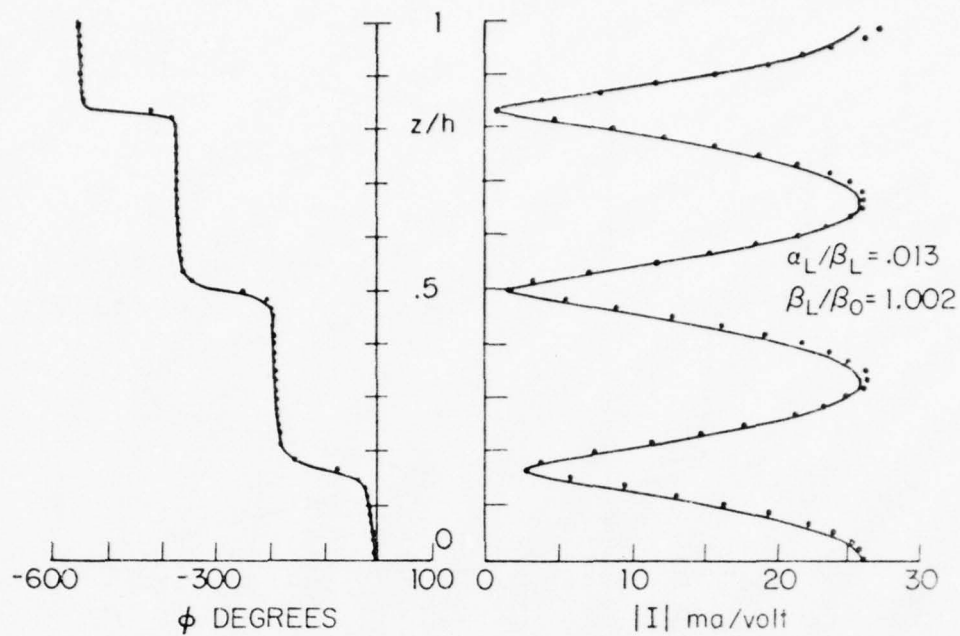


a) CURRENT DISTRIBUTION

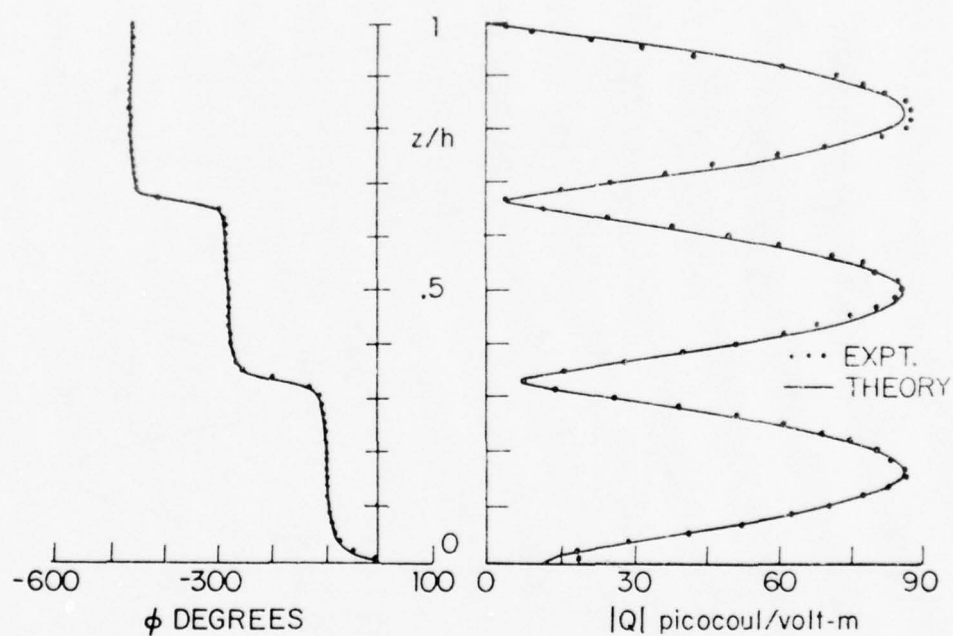


b) CHARGE DISTRIBUTION

FIG. 4d. CURRENT AND CHARGE DISTRIBUTION ON SHORT-CIRCUITED MONOPOLE OVER FRESH WATER;  $h/\lambda_0 = 1.5$  AND  $d/\lambda_0 = .1$ .  
 $a/\lambda_0 = 0.0015$ .

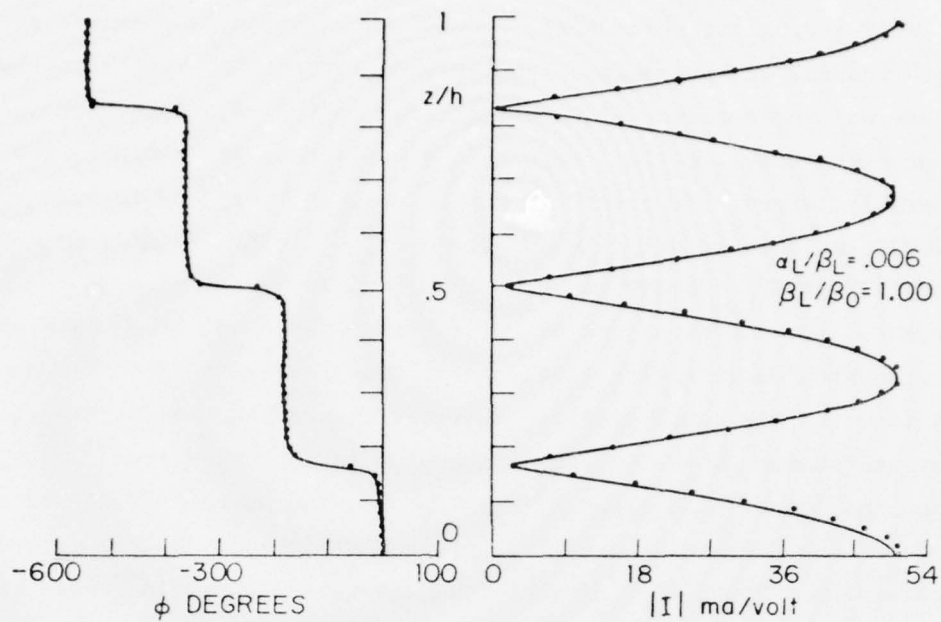


a) CURRENT DISTRIBUTION

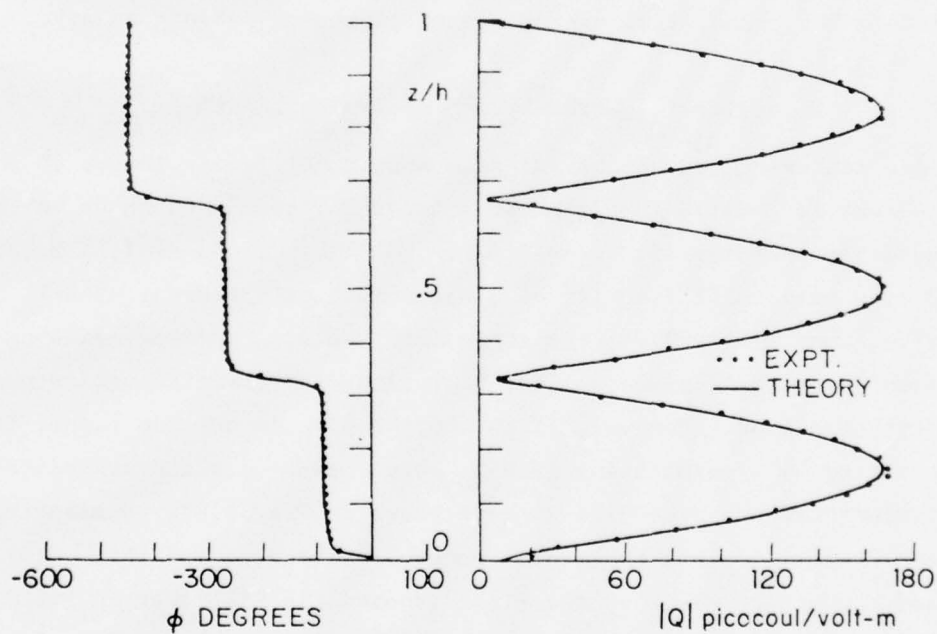


b) CHARGE DISTRIBUTION

FIG. 4e. CURRENT AND CHARGE DISTRIBUTION ON SHORT-CIRCUITED MONOPOLE OVER FRESH WATER;  $h/\lambda_0 = 1.5$  AND  $d/\lambda_0 = 1.3$ .  $a/\lambda_0 = 0.0015$ .



a) CURRENT DISTRIBUTION



b) CHARGE DISTRIBUTION

FIG. 4f. CURRENT AND CHARGE DISTRIBUTION ON SHORT-CIRCUITED MONOPOLE OVER FRESH WATER;  $h/\lambda_0 = 1.5$  AND  $d/\lambda_0 = .25$ .  $a/\lambda_0 = 0.0015$ .



With  $d/\lambda_0 = 0.01$  for which  $\alpha_L/\beta_L = 0.147$ , the current and charge per unit length in Fig. 4a have a low standing-wave ratio (SWR) with a nearly linear phase as a consequence of close coupling to the adjacent water and the transfer of much power into it. With  $d/\lambda_0 = 0.02$  and  $\alpha_L/\beta_L = 0.096$ , the SWR is considerably larger. It rises rapidly as  $d/\lambda_0$  is increased to 0.05 with  $\alpha_L/\beta_L = 0.039$  and then to  $d/\lambda_0 = 0.10$  with  $\alpha_L/\beta_L = 0.018$ . Finally when  $d/\lambda_0 = 0.13$  and 0.25,  $\alpha_L/\beta_L = 0.013$  and 0.006, the SWR is high - near 30 for the larger height. The distributions of current and charge are like those on a low-loss transmission line with little power transferred to the water and radiation into the air quite small. The rapid changes in the distributions of current and charge as the height of the wire is increased from  $d/\lambda_0 = 0.01$  to 0.05 and the slower changes as  $d/\lambda_0$  is further increased to 0.25 are a consequence of the decreasing coupling between the antenna and the water-filled half-space. The effect of the proximity to the water increases rapidly when  $d/\lambda_0$  is smaller than about 0.05 as seen in Fig. 3 in the graphs for  $\alpha_L/\beta_0$  and  $\beta_L/\beta_0$ . Since the water is acting like a dielectric, most of the power transferred to it from the antenna is not dissipated locally in conduction currents but transmitted over large distances as radiant energy.

## 2. Horizontal-Wire Antenna of Finite Length

When a center-driven horizontal-wire antenna of finite length  $2h$  and with open ends is located in air above a dense half-space as shown in Fig. 5(a), radiation into the air is negligible only when  $|k_2 d| \ll 1$ , i.e., the height  $d$  is a very small fraction of a wavelength of the order of  $d/\lambda_0 < 0.05$ . Furthermore, when  $d/\lambda_0 > 0.05$ , radiation into the air, unlike radiation into the adjacent dense half-space, cannot be included in the attenuation constant as a distributed load. However, if the height  $d/\lambda_0$  is not too large, it can be approximated by a terminating load  $Z_s$  across each open end as indicated in the equivalent transmission-line circuit shown in Fig. 5(b). Similarly, the equivalent circuit for the horizontal monopole with open end [Fig. 2(b) with  $Z_s = 0$  and the ground plane on the right removed] is like that in Fig. 5(b) with the transmission-line section to the left of the generators replaced by a short circuit. The current distribution  $I(z)$  on the terminated line remaining on the right in Fig. 5(b) is [3]:

$$I(z) = jV_0 \sin[k_L(h - |z|) - j\theta_s]/Z_c \cos(k_L h - j\theta_s) \quad (3)$$



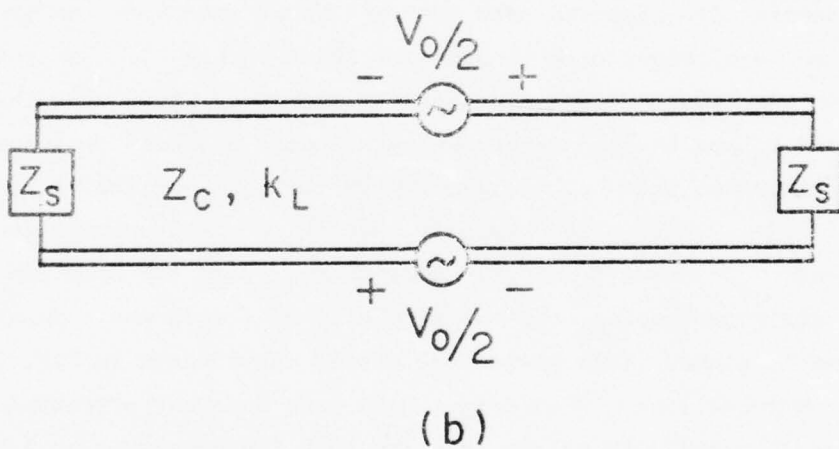
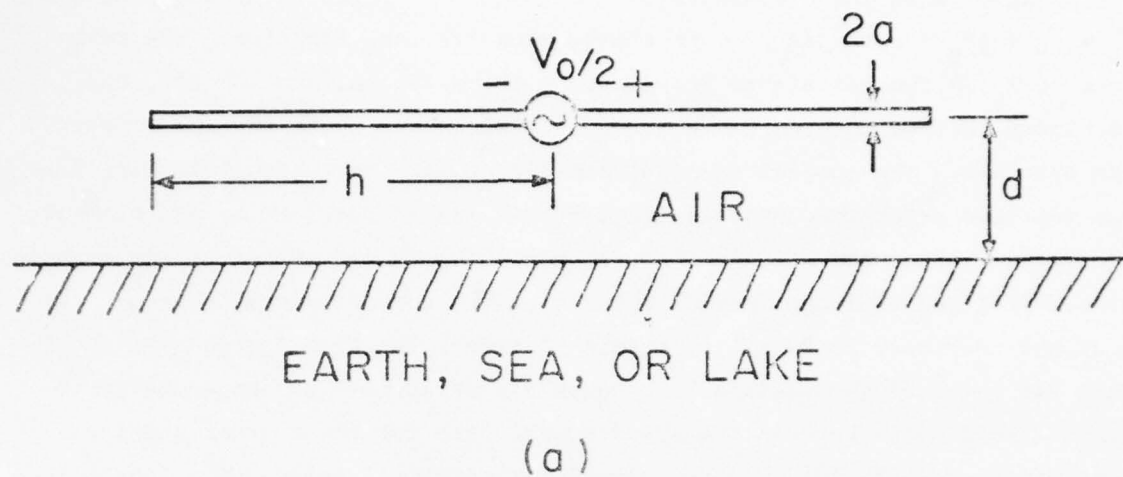


FIG. 5 (a) HORIZONTAL-WIRE ANTENNA OF FINITE LENGTH PLACED IN AIR OVER A DENSE HALF-SPACE. (b) MATHEMATICALLY APPROXIMATELY EQUIVALENT, TERMINATED LOSSY TRANSMISSION LINE.

(For the center-driven line in Fig. 5(b) the same formula applies with an added factor 2 in the denominator.) In (3)  $h$  is the length of the line and  $\theta_s = \rho_s + j\phi_s \equiv \coth^{-1}(Z_s/Z_c)$  is the complex terminal function. The real part of  $Z_s$  is the resistance associated with radiation into the air, the imaginary part is the reactance associated with the capacitive end effect at the open end. The complex terminal function  $\theta_s$  for the circuit in Fig. 5(b) has not been determined analytically, but it can be obtained by measurement. The current along the antenna shown in Fig. 5(b) is determined by six quantities, viz., the real and imaginary parts of the complex wave number  $k_L$ , the real and imaginary parts of the complex terminal function  $\theta_s$ , and the amplitude and phase of the voltage  $V_0$ . These six parameters can be adjusted to yield a good match between the experimental data for the current and the theoretical formula (3). (Alternatively, theoretical values of  $\alpha_L$  and  $\beta_L$  can be used and the other four parameters adjusted to obtain a good fit.)

The values of  $\alpha_L$ ,  $\beta_L$ ,  $\rho_s$  and  $\phi_s$  obtained from the currents measured on a horizontal monopole with open end over the same water used with the monopole terminated in an ideal short circuit are also shown in Fig. 3. The points calculated from the measured data are shown by crosses. It is seen that the values of  $\beta_L$  and  $\alpha_L$  are in good agreement with theory and with measurements for the short-circuited antenna. However, with the open end the values of  $\rho_s$  and  $\phi_s$  shown in Fig. 3 were also obtained. With a short-circuiting ground plane at the end,  $\rho_s = 0$  and  $\phi_s = \pi/2$ . Note that if with the open end radiation into the air were ignored, the quantity  $\alpha'_L = \alpha_L + \rho_s/h$  would appear as the attenuation constant. This yields the dotted curve shown in Fig. 3 instead of that in solid line. When  $d/\lambda_0 > 0.05$ , the apparent attenuation constant  $\alpha'_L$  increases rapidly to values that are much larger than  $\alpha_L$ . A similar error would be made in  $\beta_L$  if  $\beta'_L = \beta_L + \phi_s/h$  were treated as the phase constant. It is clear, therefore, that when a horizontal-wire antenna has open ends or is terminated in any impedance other than the ideal short circuit provided by large ground planes, the more general formula (3) for the current must be used. This reduces to (2) when  $\theta_s \pm 0$ , as when  $d/\lambda_0$  is sufficiently small. Typical graphs of the currents on a resonant and a traveling-wave antenna are shown in Figs. 6 and 7, respectively. The antenna was  $1.0\lambda_0$  in length with a resistor and quarter-wave section added for the traveling-wave case. Theory and measurements are again in excellent agreement.

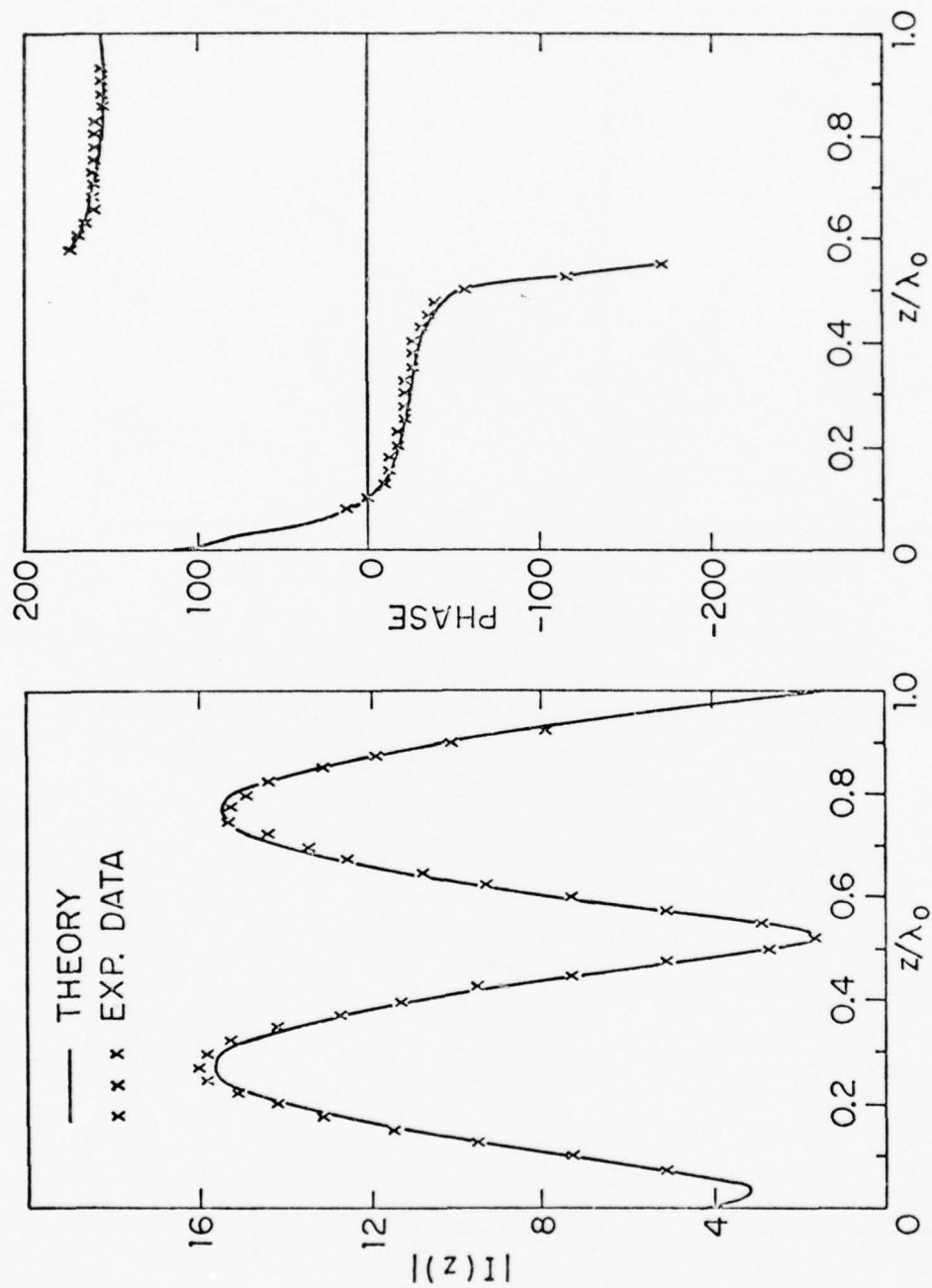


FIG. 6 MEASURED CURRENT DISTRIBUTION AND BEST FITTING THEORETICAL CURVE FOR  $\sigma = 0.092$  Si/m,  $d/\lambda_0 = 0.0775$ , WITHOUT LOAD.  $a/\lambda_0 = 0.0015$ .

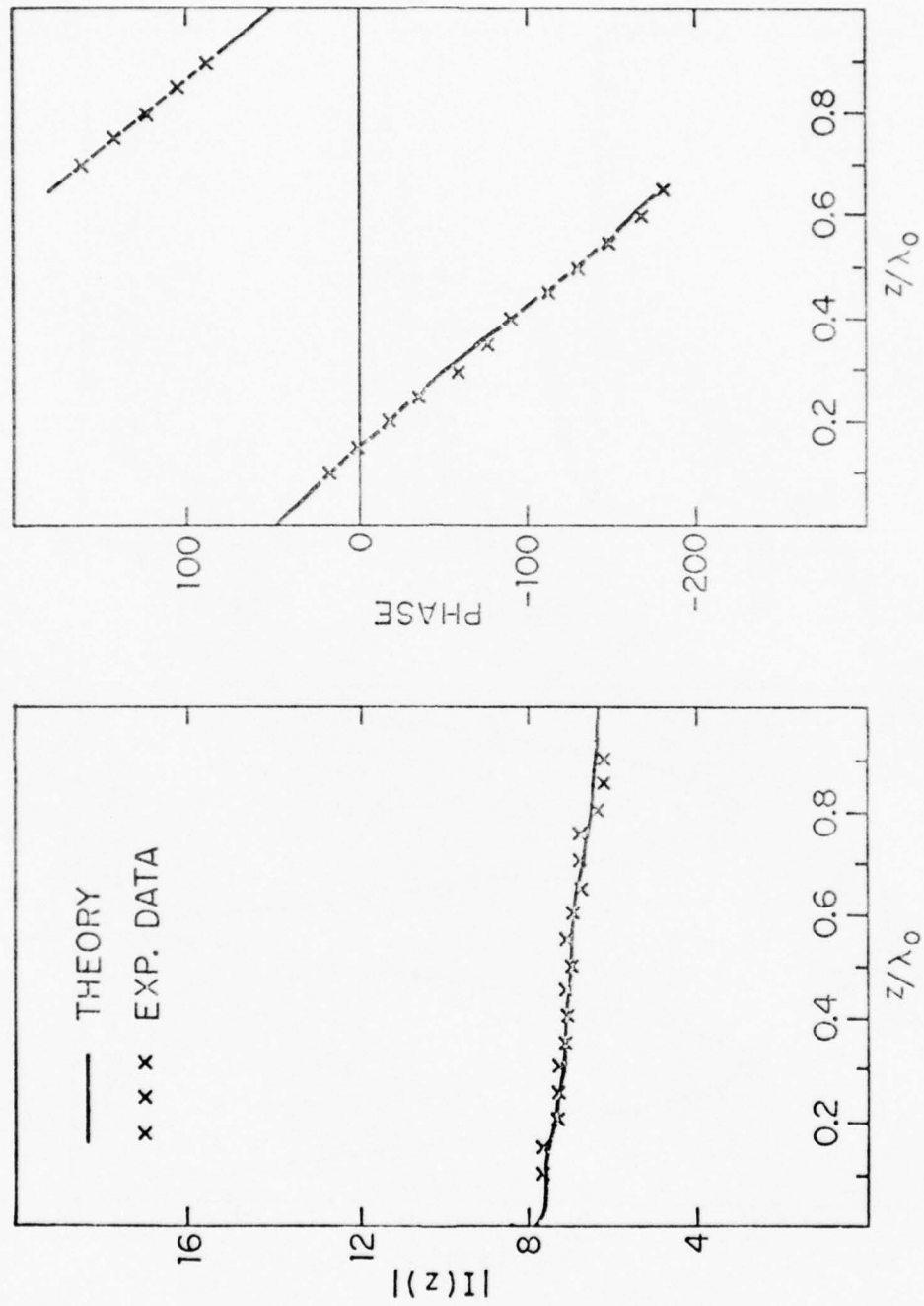


FIG. 7 MEASURED CURRENT DISTRIBUTION AND BEST FITTING THEORETICAL CURVE FOR  $\sigma = 0.092$  SI/M,  $d/\lambda_0 = 0.0775$ , WITH RESISTOR LOAD (270 ohm d.c. RESISTOR PLUS QUARTER-WAVELENGTH SECTION OF WIRE)  $a/\lambda_0 = 0.0015$ .



Graphs of the theoretical values of  $\alpha_L/\beta_0$  and  $\beta_L/\beta_0$  for an infinitely long antenna and the values determined from the measured currents when  $h/\lambda_0 = 1.5$  for a monopole with open end over salt water are shown in Fig. 8 together with the associated terminal functions  $\rho_s$  and  $\phi_s$ . The quantity  $(\alpha_L/\beta_0 + \rho_s/\beta_0 h)$  is also shown. The agreement for  $\alpha_L/\beta_0$  is good for the entire range  $0.01 \leq d/\lambda_0 \leq 0.15$ ; the difference between the theoretical and measured values of  $\beta_L/\beta_0$  is near 1%.

### 3. Description of the Experiment

Distributions of current and charge per unit length were measured along an antenna extended horizontally from a vertical aluminum ground plane at a height  $d$  over a large tank filled with water as sketched in Fig. 9. The antenna was variable in length and made of brass tubing 3 mm in outside diameter. Its end was left open for studying a resonant antenna; it was connected to a suitable resistor (220, 270 or 330 ohms) in series with a quarter-wavelength section of brass tubing to obtain a traveling-wave antenna, and directly to a second vertical metal ground plane when a short circuit was needed. In order to make reflections from the walls and bottom of the tank negligibly small, sufficient salt was mixed with the water. With  $\sigma = 0.092$  Si/m - a value only slightly higher than the conductivity of some lakes, e.g., Mystic Lake near Cambridge, Mass. with  $\sigma = 0.06$  Si/m - the tank behaved substantially like a dielectric at the operating frequency  $f = 300$  MHz since the loss tangent  $p = \sigma/\omega\epsilon = 0.067$ . More salt was added to make  $\sigma = 3.9$  Si/m for measurements over the equivalent of sea water. The height  $d$  of the antenna was varied over the values  $d/\lambda_0 = 0.01, 0.02, 0.05, 0.1, 0.13$  and  $0.25$ . Details of the construction of the ground plane and the water tank are given elsewhere [4].

### 4. Discussion of Results and Conclusion

Excellent agreement between the generalized transmission-line formula and measured data has been obtained for the antenna terminated both in a ground plane and in an open end. With the former, radiation into the air is negligible when  $d/\lambda_0 < 0.25$  and  $h = 1.5\lambda_0$ , and virtually the entire transfer of power is from the antenna into the adjacent electrically dense medium where it propagates as outward-traveling electromagnetic waves when the

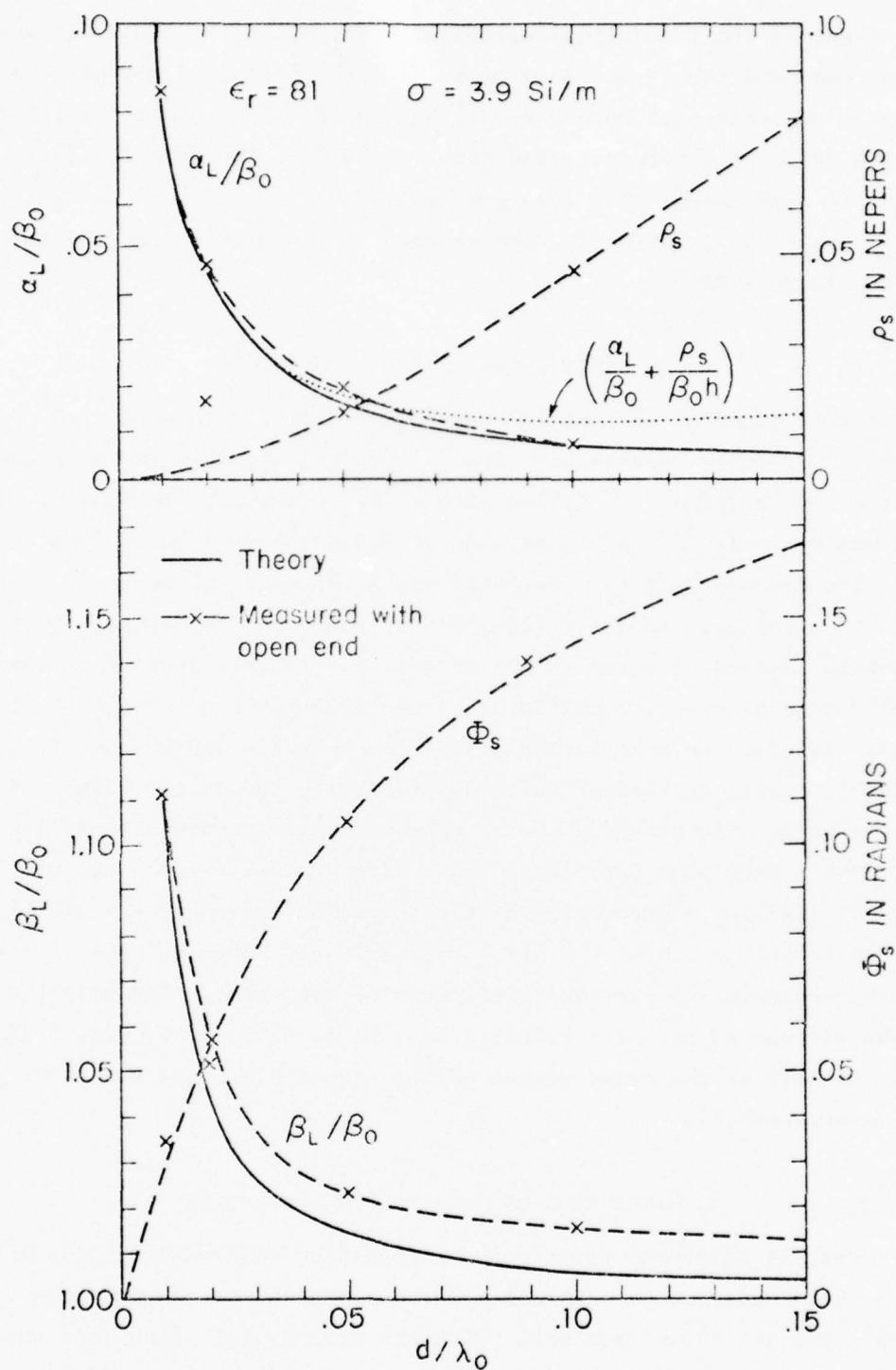


FIG. 8 PHASE AND ATTENUATION CONSTANTS, TERMINAL PHASE AND ATTENUATION FUNCTIONS FOR OPEN-CIRCUITED HORIZONTAL MONOPOLE OVER SALT WATER.  $a/\lambda_0 = 0.0015$ .

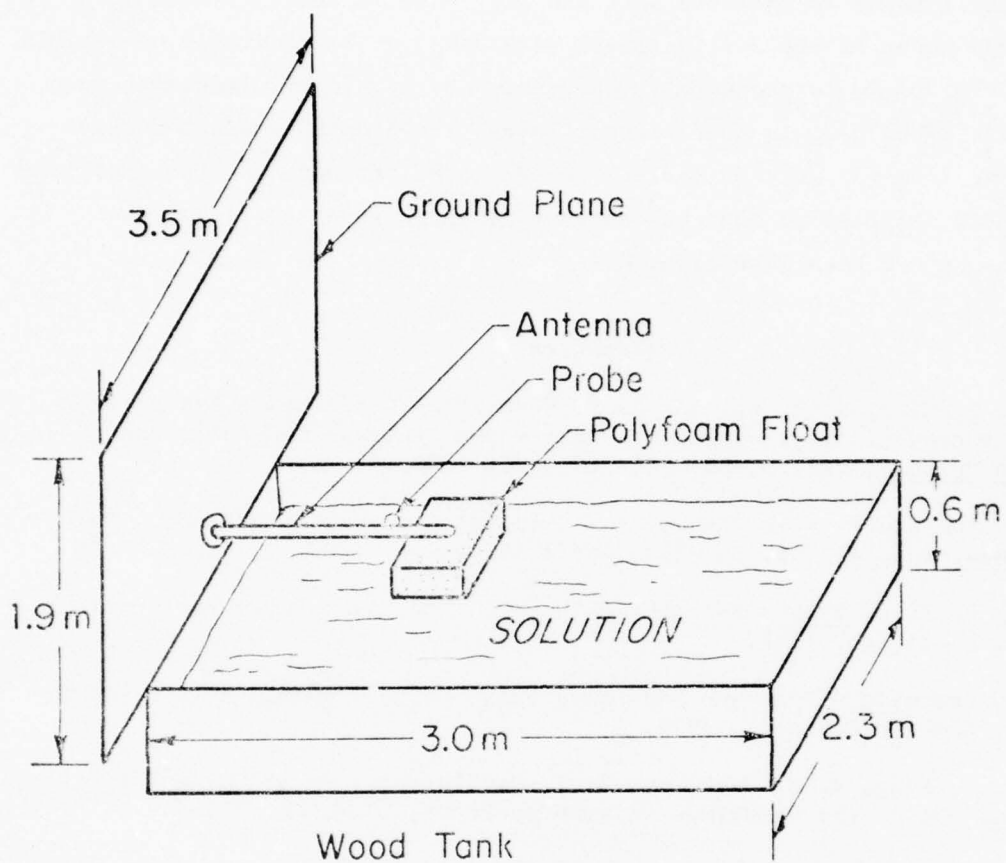


FIG. 9 SKETCH OF EXPERIMENTAL SETUP SHOWING WATER TANK, GROUND PLANE AND ANTENNA.

dielectric properties of the medium dominate ( $\sigma/\omega\epsilon \ll 1$ ) and is dissipated by local conduction currents when the conducting properties are sufficiently large ( $\sigma/\omega\epsilon \gg 1$ ). With the latter, a small but significant fraction of the power in the antenna is radiated into the air. The relative importance of the radiated power in the air increases with  $d/\lambda_0$ ; it is generally negligible when  $d/\lambda_0 \leq 0.05$  and is adequately represented by a terminal impedance when  $d/\lambda_0 \leq 0.15$ . When  $d/\lambda_0$  is sufficiently large, the simple terminated transmission-line form (3) for the current ceases to be adequate and the distribution characteristic of an isolated antenna is approached [5], [6]. The transition has not been investigated.

## 5. References

- [1] R. W. P. King, T. T. Wu, and L. C. Shen, "The horizontal-wire antenna over a conducting or dielectric half-space: Current and admittance," Radio Science, vol. 9, pp. 701-709, July 1974.
- [2] K.-M. Lee and R. W. P. King, "The terminated insulated antenna," Radio Science, vol. 11, pp. 367-373, April 1976.
- [3] R. W. P. King, Transmission-Line Theory. New York: Dover Publications, 1965, p. 85, eq. (16).
- [4] R. M. Sorbello, "Beverage Wave Antennas," Ph.D. Thesis, Harvard University, Cambridge, Mass., 1976.
- [5] R. W. P. King, R. B. Mack, and S. S. Sandler, Arrays of Cylindrical Dipoles. New York: Cambridge University Press, 1968, Ch. II.
- [6] C. L. Chen and T. T. Wu, "Theory of the long dipole antenna," Ch. 10 in Antenna Theory, Part I, R. E. Collin and F. J. Zucker, Eds. New York: McGraw-Hill, 1969, pp. 421-457.



BEST AVAILABLE COPY

### III. THE TWO-ELEMENT BEVERAGE ARRAY

A theoretical and experimental investigation of the circuit properties of coupled horizontal-wire antennas above an electrically dense dissipative half-space has been completed. In Section A the theory developed for two coupled parallel horizontal antennas is presented and compared with measurements made on coupled antennas over fresh- and salt-water solutions. Since the validity of the simple theoretical formulas is confirmed, the originally planned measurements over an actual earth were deemed unnecessary. A brief description of measurements made on two coupled collinear Beverage antennas then follows in Section B.

#### A. Coupled Horizontal-Wire Antennas Over a Conducting or Dielectric Half-Space

The properties of two coupled horizontal-wire antennas over a homogeneous isotropic half-space are derived. The complex wave number, distribution of current, and admittance of the antennas are determined for symmetrical and antisymmetrical excitations. The wave number of the half-space is assumed to be large in magnitude compared with that in air. The theory of the coupled horizontal-wire antennas is extended to take account of radiation into the air and so enlarge its range of validity while preserving the transmission-line form. This is accomplished by incorporating the effects of this radiation and of the capacitive end correction for the open end in a lumped terminal impedance which is conveniently represented by a complex terminal function. This function is determined from a least-squares fit of the measured and the theoretical current distributions.

## 1. INTRODUCTION

In a recent paper [King et al., 1974] the properties of a horizontal-wire antenna over a homogeneous isotropic half-space are determined when the complex wave number characteristic of the half-space is large in magnitude compared with the real wave number of the air. These solutions are obtained from those of the eccentrically insulated dipole in a general medium [Wu et al., 1975] through a limiting process. When two center-driven dipole antennas are placed parallel to one another and to a conducting or dielectric half-space at the same height  $d$  above it and with a distance  $L$  between them as shown in Fig. 1, the currents and charges in each antenna not only interact with the induced currents and charges in the dissipative half-space but also with the currents and charges in the other antenna. The exact calculation of the interaction is difficult except when the half-space is perfectly conducting. In this case, with the help of image theory the problem reduces to that of four identical parallel antennas at the corners of a rectangle with the dimensions  $2d$  and  $L$ . The antennas separated by the distance  $2d$  are driven by equal and opposite generators [King, 1956]. When the half-space is not perfectly conducting, an exact analysis is complicated. However, if the method of solution in the previous paper [Wu et al., 1975] is used along with a limiting process similar to that used in [King et al., 1974], an approximate solution for the currents in the coupled antennas can be obtained. The same limitation on the wave numbers of the media is assumed.

## 2. APPROXIMATE SOLUTION FOR THE CURRENTS IN COUPLED INSULATED ANTENNAS

A solution for the current in a center-driven, eccentrically insulated antenna has been obtained [Wu et al., 1975]. A similar structure with two conductors in a circular cylindrical insulation is shown in Fig. 2. The radius of the insulation is  $b$ , that of each conductor is  $a$ . The axis of each conductor is at a distance  $D$  from the axis of the insulator or at a distance  $d = b - D$  from its surface. The radii to the axes of the two conductors subtend an angle  $2\theta_0$ . The wave number characteristic of the insulating material is  $k_2 = \beta_2 + i\alpha_2 = \omega[\mu(\epsilon_2 + i\sigma_2/\omega)]^{1/2} = \omega(\mu\tilde{\epsilon}_2)^{1/2}$ . The wave number characteristic of the ambient medium in the range  $b < r < \infty$  is  $k_4 = \beta_4 + i\alpha_4 = \omega[\mu(\epsilon_4 + i\sigma_4/\omega)]^{1/2} = \omega(\mu\tilde{\epsilon}_4)^{1/2}$ , where  $\beta_4$  is the real phase constant and  $\alpha_4$  the real attenuation constant. It is assumed in the analysis that the

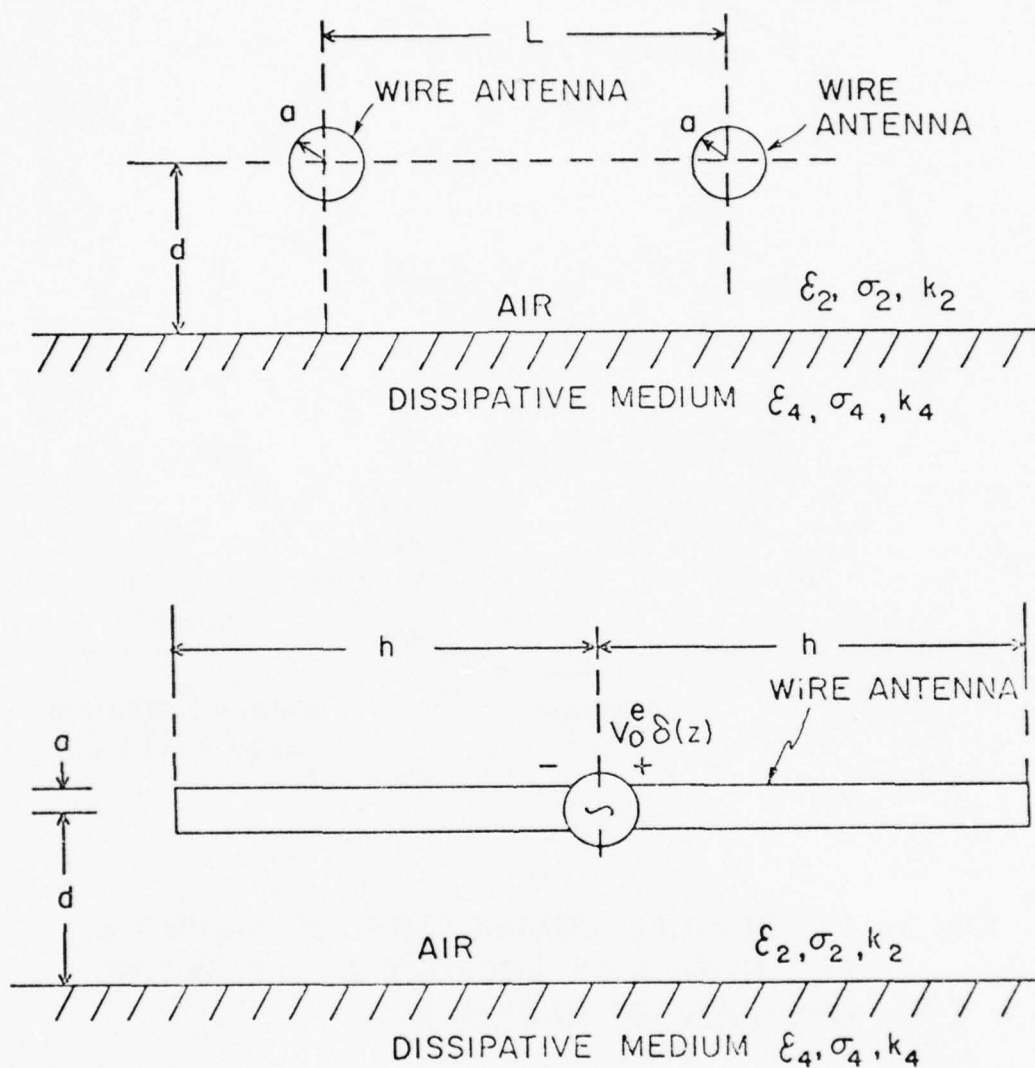


FIG. 1 COUPLED HORIZONTAL WIRES OVER A DISSIPATIVE OR DIELECTRIC HALF SPACE.

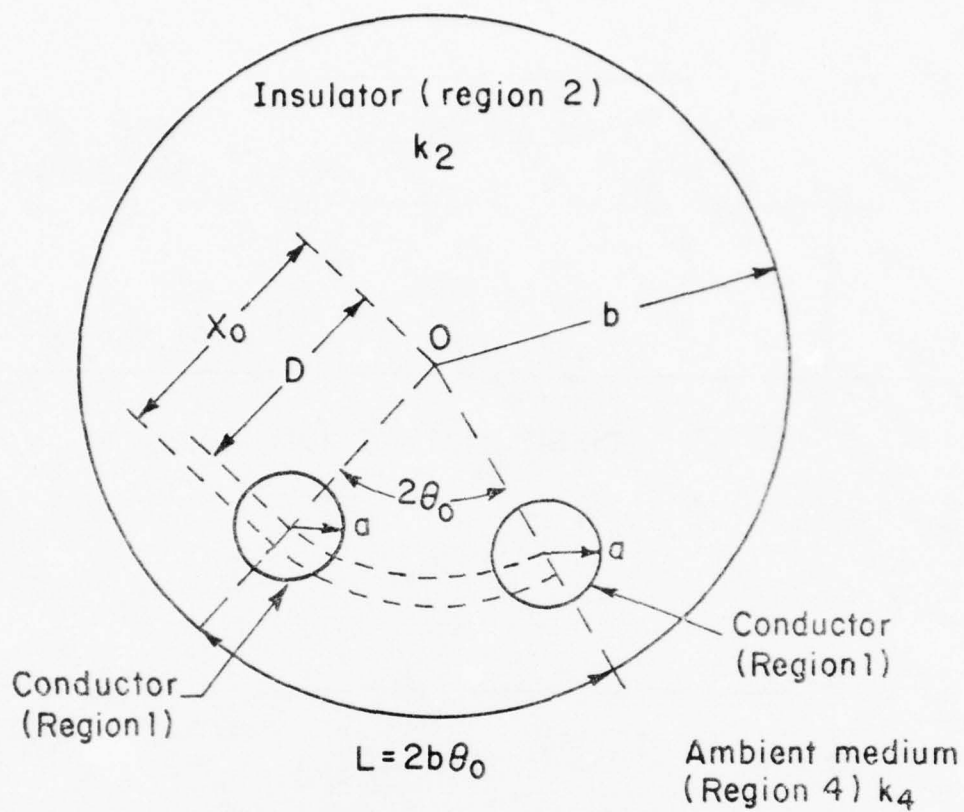


FIG. 2 CYLINDRICAL CONDUCTORS OF RADIUS  $a$  ECCENTRICALLY LOCATED IN DIELECTRIC CYLINDER OF RADIUS  $b$ .



following conditions are satisfied:

$$|k_4^2| \gg |k_2^2| \quad ; \quad |k_2 d| \ll 1 \quad (1)$$

$$L = 2b\theta_0 > d \gg a \quad (2)$$

Let two infinitely long conductors be considered first. The electric field on each wire can be obtained from a superposition of 1) the field on the wire due to the current in the wire itself, and 2) the field on the wire due to the current in the second wire. The Fourier transform of the first electric field is [Wu et al., 1975, Eq. (13)]:

$$\bar{E}_{z1} = (i\bar{I}\Omega_a/2\pi\omega\epsilon_2)[k_2^2(1 + \Delta_0/k_4 b\Omega_a) - \zeta^2] \quad (3)$$

where

$$\Omega_a = \cosh^{-1} \left( \frac{a^2 + b^2 - D^2}{2ab} \right) \quad (4)$$

$$\Delta_0 = \frac{H_0^{(1)}(k_4 b)}{H_1^{(1)}(k_4 b)} + 2 \sum_{m=1}^{\infty} \left( \frac{Dx_0}{b^2} \right)^m \frac{H_m^{(1)}(k_4 b)}{H_{m+1}^{(1)}(k_4 b)} \quad (5)$$

with

$$x_0 = (1/2D)\{(b^2 + D^2 - a^2) - [(b^2 + D^2 - a^2)^2 - 4b^2 D^2]^{1/2}\} \quad (6)$$

The Fourier transform of the second field is [Wu et al., 1975, Eq. (7a)]:

$$\bar{E}_{z2}^{(m)} = [(-1)^m i\bar{I}/2\pi\omega\epsilon_2][(k_2^2 - \zeta^2)\langle\Omega(r, \theta)\rangle_C + (k_2^2/k_4 b)\langle\Delta(r, \theta)\rangle_C], \quad m = 0, 1 \quad (7)$$

where  $m = 0$  applies when the two wires are driven in phase by equal voltages (symmetrical or zero-phase-sequence excitation) and  $m = 1$  applies when the two wires are driven by equal voltages  $180^\circ$  out of phase (antisymmetrical or first-phase-sequence excitation).  $\langle\Omega(r, \theta)\rangle_C$  and  $\langle\Delta(r, \theta)\rangle_C$  are average values of  $\Omega(r, \theta)$  and  $\Delta(r, \theta)$  [Wu et al., 1975, Eqs. (7b), (7c)] evaluated on a circle of radius  $a$ , centered at  $r = D$  and  $\theta = 2\theta_0$ . This circle is denoted by  $C$ , and the averages are just equal to their values at the center of the circle, in

this case at  $r = D$ ,  $\theta = 2\theta_0$ :

$$\langle \Omega(r, \theta) \rangle_C = \Omega(D, 2\theta_0) = \frac{1}{2} \ln \left[ \frac{(Dx_0)^2 - 2b^2 Dx_0 \cos 2\theta_0 + b^4}{b^2 (D^2 - 2Dx_0 \cos 2\theta_0 + x_0^2)} \right] \quad (8)$$

$$\langle \Delta(r, \theta) \rangle_C = \Delta(D, 2\theta_0) = \frac{H_0^{(1)}(k_4 b)}{H_1^{(1)}(k_4 b)} + 2 \sum_{m=1}^{\infty} \left( \frac{Dx_0}{b^2} \right)^m \frac{H_m^{(1)}(k_4 b)}{H_{m+1}^{(1)}(k_4 b)} \cos(2m\theta_0) \quad (9)$$

The total field on one wire is:

$$\begin{aligned} \bar{E}_z^{(m)} &= \bar{E}_{z1} + \bar{E}_{z2}^{(m)} \\ &= (i\bar{I}/2\pi\omega\epsilon_2) \{ k_2^2 [\Omega_a + (-1)^m \Omega(D, 2\theta_0)] - \zeta^2 [\Omega_a + (-1)^m \Omega(D, 2\theta_0)] \\ &\quad + (k_2^2/k_4 b) [\Delta_0 + (-1)^m \Delta(D, 2\theta_0)] \} \quad , \quad m = 0, 1 \end{aligned} \quad (10)$$

When the conductors are driven by unit delta-function generators at  $z = 0$ ,  $\bar{E}_z = -1$  on the wire. The substitution of this value in (10) yields the transform of the current,  $\bar{I}^{(m)}(\zeta)$ . It is

$$\bar{I}^{(m)}(\zeta) = \frac{-2\pi i \omega \epsilon_2}{(\zeta^2 - [k_L^{(m)}]^2) [\Omega_a + (-1)^m \Omega(D, 2\theta_0)]} \quad , \quad m = 0, 1 \quad (11)$$

where the phase-sequence wave numbers  $k_L^{(m)}$  are given by

$$[k_L^{(m)}]^2 = k_2^2 \left\{ 1 + \frac{\Delta_0 + (-1)^m \Delta(D, 2\theta_0)}{(k_4 b) [\Omega_a + (-1)^m \Omega(D, 2\theta_0)]} \right\} \quad , \quad m = 0, 1 \quad (12)$$

The current distribution along each of the center-driven coupled dipoles of length  $2h$  located as shown in Fig. 2 in an insulating region 2 which is immersed in a relatively dense region 4 is given by the transmission-line formula:

$$I^{(m)}(z) = \frac{-iV_0^{(m)} \sin k_L^{(m)}(h - |z|)}{2Z_c^{(m)} \cos(k_L^{(m)} h)} \quad , \quad m = 0, 1 \quad (13)$$

where  $V_0^{(m)}$  is the phase-sequence driving voltage,

$$Z_c^{(m)} = \frac{\zeta_2 k_L^{(m)} [\Omega_a + (-1)^m \Omega(D, 2\theta_0)]}{2\pi k_2}, \quad m = 0, 1 \quad (14)$$

is the phase-sequence characteristic impedance, and  $\zeta_2 = (\mu_2/\epsilon_2)^{1/2}$  is the complex wave impedance of region 2. For air  $\zeta_2 \doteq 120\pi$  ohms,  $k_2 = \omega/c$ ,  $c = 3 \times 10^8$  m/sec.

With  $m = 0$  in (12) and (14), the two conductors are driven in phase by equal emf's,  $V_1 = V_2 = V_0^{(0)}$ , and the currents are identical,  $I_1(z) = I_2(z) = I^{(0)}(z)$ . With  $m = 1$  in (12) and (14), the two conductors are driven  $180^\circ$  out of phase by equal emf's,  $V_1 = -V_2 = V_0^{(1)}$ , and the currents are equal in magnitude but oppositely directed,  $I_1(z) = -I_2(z) = I^{(1)}(z)$ . Note that these results are readily generalized to give the currents in a two-wire line in a tunnel of circular cross section [Wait, 1975].

### 3. TWO HORIZONTAL WIRES OVER A HALF-SPACE

The solution obtained in the previous section can now be used to find the properties of two horizontal wires over a half-space. The first step is to determine the quantities  $\Omega_a$ ,  $\Delta_0$ ,  $\Omega(D, 2\theta_0)$  and  $\Delta(D, 2\theta_0)$  in the limit  $b \rightarrow \infty$ ,  $D \rightarrow \infty$  with  $d = (b - D)$  fixed and finite. The first two quantities are given in [King et al., 1974]. They are

$$\Omega_a \doteq \cosh^{-1}(d/a) \doteq \ln(2d/a) \quad (15)$$

$$\Delta_0/k_4 b \doteq 2T(2k_4 d, 0) \quad (16)$$

where  $d$  is the distance from the axis of the wire in air to the plane boundary between the air (region 2) and the material half-space (region 4). Also,  $T(A, B)$  is given by Eq. (A13) in [King et al., 1974]. An equivalent form is

$$\begin{aligned} T(A, B) = & \frac{A^2 - B^2}{(A^2 + B^2)^2} - \frac{K_1(A - iB)}{A - iB} + \frac{\pi}{4(B + iA)} [Y_1(B + iA) + E_1(B + iA) - 2/\pi] \\ & - \frac{\pi}{4(B - iA)} [Y_1(B - iA) + E_1(B - iA) - 2/\pi] \end{aligned} \quad (17)$$

(The form in Eq. (A13) of [King et al., 1974] is  $T(A,B) = (A^2 - B^2)/(A^2 + B^2)^2 - K_1(A - iB)/(A - iB) + i\text{Im}[\pi/2(A - iB)][Y_1(B + iA) + E_1(B + iA) - 2/\pi]$ . This is equivalent to (17) when A and B are real. However, since the sum of integrals which yield the two equivalent expressions for  $T(A,B)$  when A and B are real is an analytic function, and the form (17) is also an analytic function, it follows by analytic continuation that (17) is also valid for complex values of A and B. Use of this fact was made by King et al. [1974] when Eq. (A17) was used to obtain the expression (28) for  $k_L$  in which  $A = 2k_4d$  is complex when  $k_4$  is complex.)

In (17)  $K_1(z)$  is the modified Bessel function of the second kind and  $Y_1(z)$  is the Bessel function of the second kind, both of order 1. The function  $E_1(z)$  is the Weber function defined by the series

$$E_1(z) = (2/\pi)(1 - z^2/3 + z^4/45 - z^6/1575 + z^8/99225 - \dots) \quad (18)$$

When this is inserted in (17) and use is made of the relation  $K_1(z) = -(\pi/2)H_1^{(1)}(iz)$ ,

$$T(A,B) = \frac{A^2 - B^2}{(A^2 + B^2)^2} + \frac{i\pi}{2} \frac{H_1^{(1)}(B + iA)}{B + iA} + \frac{\pi}{4} \left[ \frac{Y_1(B + iA)}{B + iA} - \frac{Y_1(B - iA)}{B - iA} \right] + \frac{1}{2} \sum_{n=1}^{\infty} [(B + iA)^{2n-1} - (B - iA)^{2n-1}] a_n \quad (19)$$

where  $a_1 = -1/3$  and  $a_n = -a_{n-1}/(4n^2 - 1)$ . When  $B = 0$ , (19) reduces to Eq. (A17) in [King et al., 1974]. For large arguments, i.e.,  $|B \pm iA| \gg 1$ , (19) is well approximated by

$$T(A,B) \approx (A^2 - B^2)/(A^2 + B^2)^2 - (\pi/2)^{1/2} (A - iB)^{-3/2} e^{-(A - iB)} [1 + 3/8(A - iB) - 15/128(A - iB)^2 + \dots] - (1/2) [(B + iA)^{-1} + (B + iA)^{-3} - 3(B + iA)^{-5} + 45(B + iA)^{-7} + \dots] + (1/2) [(B - iA)^{-1} + (B - iA)^{-3} - 3(B - iA)^{-5} + 45(B - iA)^{-7} + \dots] \quad (20)$$



To evaluate  $\Omega(D, 2\theta_0)$  in the limit  $b \rightarrow \infty$ ,  $D \rightarrow \infty$  with  $d$  fixed, note that  $x_0 \rightarrow (b - d) = D$ . The distance  $L$  between the two wires is related to the angle  $\theta_0$  by  $L = 2b\theta_0$ . Since  $2\theta_0 = L/b \ll 1$ , it follows that

$$\cos 2\theta_0 \approx 1 - (2\theta_0)^2/2 = 1 - L^2/2b^2 \quad (21)$$

In the limit  $b \rightarrow \infty$ ,

$$\begin{aligned} \Omega(D, 2\theta_0) &\rightarrow \frac{1}{2} \ln \left\{ \frac{D^4 - 2b^2 D^2 (1 - L^2/2b^2) + b^4}{b^2 [D^2 - 2D^2 (1 - L^2/2b^2) + D^2]} \right\} \\ &\approx \frac{1}{2} \ln(1 + 4d^2/L^2) \end{aligned} \quad (22)$$

Similarly,

$$\begin{aligned} \Delta(D, 2\theta_0) &\rightarrow \frac{H_0^{(1)}(k_4 b)}{H_1^{(1)}(k_4 b)} + 2 \sum_{m=1}^{\infty} \left( \frac{b-d}{b} \right)^{2m} \frac{H_m^{(1)}(k_4 b)}{H_{m+1}^{(1)}(k_4 b)} \cos(2m\theta_0) \\ &= \lim_{\substack{b \rightarrow \infty \\ D \rightarrow \infty}} \left\{ 1 + 2 \sum_{m=2}^{\infty} (1 - d/b)^{2m} \frac{H_{m-1}^{(1)}(k_4 b)}{H_m^{(1)}(k_4 b)} \cos[2(m-1)\theta_0] \right\} \\ &= \lim_{\substack{b \rightarrow \infty \\ D \rightarrow \infty}} \left\{ 1 + 2 \sum_{m=2}^{\infty} (1 - d/b)^{2m} \left[ \frac{m + 1 [(k_4 b)^2 - m^2]^{1/2}}{k_4 b} \right] \right. \\ &\quad \times \cos[2(m-1)\theta_0] + 2 \sum_{k_4 b}^{\infty} (1 - d/b)^{2m} \left[ \frac{m - [m^2 - (k_4 b)^2]^{1/2}}{k_4 b} \right] \\ &\quad \times \cos[2(m-1)\theta_0] \left. \right\} \end{aligned} \quad (23)$$

where use has been made of the following approximations:

$$H_{m-1}^{(1)}(k_4 b)/H_m^{(1)}(k_4 b) \approx \{m + 1 [(k_4 b)^2 - m^2]^{1/2}\}/k_4 b, \quad k_4 b > m \quad (24)$$

$$H_{m-1}^{(1)}(k_4 b) / H_m^{(1)}(k_4 b) \approx \{m - [m^2 - (k_4 b)^2]^{1/2}\} / k_4 b, \quad k_4 b < m \quad (25)$$

The sum in the expression (23) can be converted into integrals with the substitutions  $x = m/k_4 b$ ,  $dx = 1/k_4 b$ . Also,

$$(1 - d/b)^{2m} = \exp(-2md/b) = \exp(-2xk_4 d) \quad (26)$$

$$\frac{m + i[(k_4 b)^2 - m^2]^{1/2}}{k_4 b} = x + i(1 - x^2)^{1/2} \quad (27)$$

$$\frac{m - [m^2 - (k_4 b)^2]^{1/2}}{k_4 b} = x - (x^2 - 1)^{1/2} \quad (28)$$

$$\cos[2(m-1)\theta_0] = \cos[(m-1)L/b] = \cos[k_4 L (\frac{m}{k_4 b} - \frac{1}{k_4 b})] \doteq \cos(k_4 Lx) \quad (29)$$

With  $A = 2k_4 d$ ,  $B = k_4 L$  and (26)-(29), it follows that (23) becomes

$$\begin{aligned} \Delta(D, 2\theta_0) = 1 + 2k_4 b \{ & \int_0^1 [x + i(1 - x^2)^{1/2}] e^{-Ax} \cos Bx \, dx \\ & + \int_1^\infty [x - (x^2 - 1)^{1/2}] e^{-Ax} \cos Bx \, dx \} \end{aligned} \quad (30)$$

In the limit  $k_4 b \rightarrow \infty$ , the first term vanishes and from Appendix A of [King et al., 1974] (30) yields

$$\Delta(D, 2\theta_0) / k_4 b = 2T(2k_4 d, k_4 L) \quad (31)$$

where  $T(A, B)$  is given by (17).

The determination of  $\Omega_a$ ,  $\Omega(D, 2\theta_0)$ ,  $\Delta_0/k_4 b$ , and  $\Delta(D, 2\theta_0)/k_4 b$  is now complete. Substitution of these quantities given, respectively, by (15), (22), (16) and (31) into (12) - (14) gives the wave number  $k_L^{(m)}$ , the current distribution  $I^{(m)}(z)$  in the antenna, and the characteristic impedance  $Z_c^{(m)}$  for this structure.

#### 4. NUMERICAL RESULTS

The propagation constant  $k_L^{(m)}$  given by (12) has been calculated for a pair of wires with equal radii  $a = 1.5$  mm, excited by a source operating at the frequency  $f = 300$  MHz. The wires are placed in air [so that  $k_2 = \omega(\mu_0\epsilon_0)^{1/2}$  and  $\zeta_2 = (\mu_0/\epsilon_0)^{1/2} \approx 120\pi$  ohms are both real] a distance  $d$  above a half-space with  $d/\lambda_2$  ranging from 0.025 to 0.13;  $\lambda_2 = 2\pi/k_2$  is the wavelength in air. The wires are separated by a distance  $L$  ranging from  $0.1\lambda_2$  to  $1.2\lambda_2$ .

The normalized complex wave number  $k_L^{(m)}/k_2 = \beta_L^{(m)}/k_2 + i\alpha_L^{(m)}/k_2$  is shown in Fig. 3 for the case when the lower medium is fresh water characterized by  $\sigma = 0.09$  Si/m,  $\mu = \mu_0$  and  $\epsilon_r = 81$ . Note that both the real propagation constant  $\beta_L^{(m)}$  and the attenuation constant  $\alpha_L^{(m)}$  are sensitive to the spacing and the relative phase of the two currents on the wire. The phase and attenuation constants for the first-phase-sequence or antisymmetrical mode are always smaller than those for the zero-phase-sequence or symmetrical mode. A similar result has been obtained by Wait [1975] for a pair of wires placed close to the walls of a tunnel.

The normalized phase and attenuation constants,  $\beta_L^{(m)}/k_2$  and  $\alpha_L^{(m)}/k_2$ , are shown in Fig. 4 for the case when the lower medium is sea water characterized by  $\sigma = 4.2$  Si/m,  $\mu = \mu_0$  and  $\epsilon_r = 81$ . It is observed that  $\beta_L^{(m)}/k_2$  is quite comparable to the corresponding values for fresh water, whereas  $\alpha_L^{(m)}/k_2$  is smaller by approximately a factor 2 in the presence of the sea water than in the presence of the less conducting and predominantly dielectric fresh water. Actually, for the same current in the wires, about twice the power can be transferred to the fresh water in which it propagates outward as radiant energy than to the sea water in which it is rapidly dissipated as heat.

#### 5. GENERALIZATION OF THE THEORY TO GREATER ANTENNA HEIGHTS

The theory of the horizontal-wire antenna [King et al., 1974] as derived from the theory of the eccentrically insulated antenna [Wu et al., 1975] implicitly neglects radiation into the air (region 2) as compared with the power transferred and radiated through or dissipated in the earth (region 4). This is an excellent approximation when the inequality  $|k_2 d| \ll 1$  is satisfied. For antennas with open ends this condition is quantitatively given by

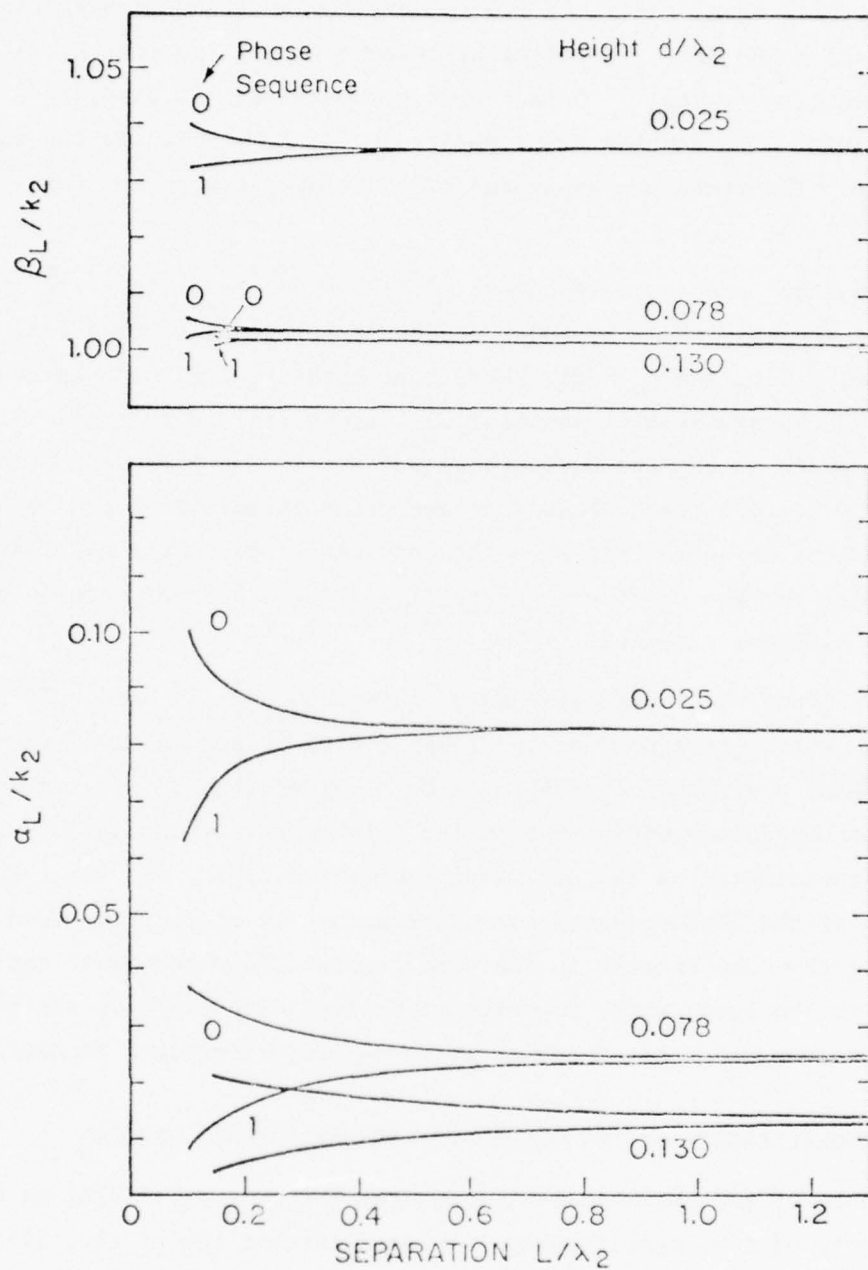


FIG. 3 NORMALIZED COMPLEX WAVE NUMBERS  $k_L/k_2 = \beta_L/k_2 + i\alpha_L/k_2$  FOR COUPLED ANTENNAS OVER LAKE WATER WITH  $\sigma = 0.09$  Si/m,  $\epsilon_r = 81$

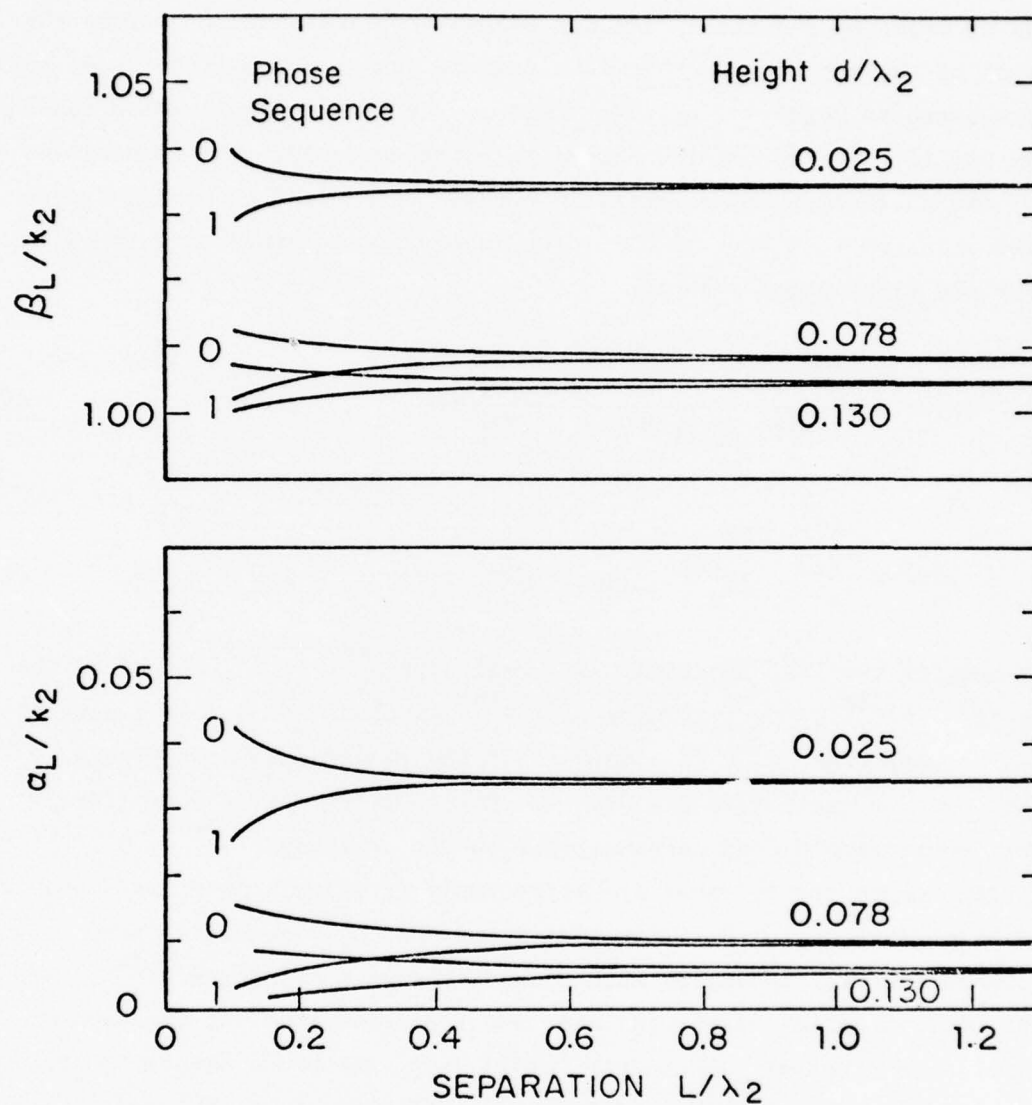


FIG. 4 NORMALIZED COMPLEX WAVE NUMBER  $k_L/k_2 = \beta_L/k_2 + i\alpha_L/k_2$  FOR COUPLED ANTENNAS OVER SALT WATER WITH  $\sigma = 4.2 \text{ Si/m}$ ,  $\epsilon_r = 81$ .



$k_2 d \leq 0.3$  or  $d/\lambda_2 \leq 0.05$ . The present formulation of the theory of coupled horizontal-wire antennas involves the same restriction for the same reason.

In a recent paper [Sorbello et al., 1977] it is shown that approximate account can be taken of radiation into region 2 from a single horizontal-wire antenna by means of a suitably defined terminating impedance  $Z_s$  across the open ends of the antenna and that when this is done the condition  $|k_2 d| \ll 1$  can be relaxed to  $|k_2 d| \leq 1$  or  $d/\lambda_2 \leq 0.16$ . The same generalization can be carried out for the two coupled horizontal-wire antennas. The generalized form of the phase-sequence currents in the two antennas when center-driven with the voltages  $V_1 = V_2 = V_0^{(0)}$  for the zero-phase sequence or  $V_1 = -V_2 = V_0^{(1)}$  for the first-phase sequence is

$$I^{(m)}(z) = \frac{-iV_0^{(m)} \sin[k_L^{(m)}(h - |z|) + i\theta_s^{(m)}]}{2Z_c^{(m)} \cos(k_L^{(m)}h + i\theta_s^{(m)})}, \quad m = 0, 1 \quad (32)$$

where

$$\theta_s^{(m)} = \rho_s^{(m)} - i\phi_s^{(m)} \equiv \coth^{-1}(Z_s^{(m)}/Z_c^{(m)}), \quad m = 0, 1 \quad (33)$$

is the complex terminal function. Its real part  $\rho_s^{(m)}$  takes account of the dissipation in  $Z_s^{(m)}$ , its imaginary part  $\phi_s^{(m)}$  involves the reactive part of  $Z_s^{(m)}$ . For open ends,  $\rho_s^{(m)}$  is a measure of the radiation into region 2,  $\phi_s^{(m)}$  corrects for the capacitive end effect. For short-circuited ends (ideally infinite conducting planes perpendicular to the antennas),  $\rho_s^{(m)} = 0$ ,  $\phi_s^{(m)} = \pi/2$ . With images the antennas are effectively infinitely long and there is no radiation into region 2. With terminated ends  $Z_s^{(m)}$  consists, for example, of a lumped resistor in series with a quarter-wave monopole and  $\rho_s^{(m)}$  takes account of dissipation in the resistor and radiation from the open-ended monopole. The terminal functions  $\rho_s$  and  $\phi_s$  for both phase sequences are closely related to the complex reflection coefficient  $\Gamma_s = |\Gamma_s| \exp(-i\psi_s)$  at the ends of the antenna. Specifically,  $|\Gamma_s| = \exp(-2\rho_s)$  and  $\psi_s = -2\phi_s$ .

It is shown in [Sorbello et al., 1977] that the theoretical values of the complex wave number  $k_L = \beta_L + i\alpha_L$  are in excellent agreement with measured values for the single antenna over the electrically dense half-space, region 4. It is reasonable to assume that the same is true for the coupled antennas. Hence, the values  $k_L^{(m)} = \beta_L^{(m)} + i\alpha_L^{(m)}$  and  $Z_c^{(m)}$  with  $m = 0, 1$  are

calculated from (12) and (14) for substitution in (32). It follows that the theoretical normalized distribution of current is completely determined except for the unknown values of  $\theta_s^{(m)} = \rho_s^{(m)} - i\phi_s^{(m)}$ . Unfortunately, no method has yet been developed for determining these theoretically. Accordingly, they are evaluated with a curve-fitting technique based on the method of least-square errors from experimentally and theoretically obtained current distributions. This is discussed following a brief description of the measurement of current distributions.

## 6. DESCRIPTION OF THE EXPERIMENT

Current distributions were measured on coupled antennas placed over a large indoor water tank. A sketch of the experimental facility is shown in Fig. 5; Fig. 6 shows the block diagram of the setup. The antennas are made of brass tubing with 3 mm outside diameter. The current probe travels along one of the antennas and the signal is led through a coaxial cable inside the brass tube. Both antennas are one meter long when operated with open ends. With terminated ends, each load consists of a resistor (with d.c. resistances of 220, 270 and 330 ohms, respectively, for heights  $d/\lambda_2 = 0.025, 0.0775$  and  $0.13$ ) and a quarter-wavelength section of brass tubing.

Salt was mixed with the water in the tank to yield a conductivity of  $\sigma = 0.09$  Si/m, which was later increased to  $\sigma = 4.2$  Si/m for a second set of measurements. The relative permittivity of the solution was  $\epsilon_r = 81$ . Three values of  $d$ , the height of each antenna above the surface of the water, were used in the experiment, namely,  $0.025, 0.0775$  and  $0.13$  m. The distance  $L$  between the two antennas was varied to include the following six values:  $0.23, 0.30, 0.40, 0.50, 0.66$  m, and infinity (single antenna). Details of the construction of the ground plane, the water tank, and discussions of their experimental characteristics are given elsewhere [Sorbelli, 1976].

The experiment was carried out at  $f = 300$  MHz. The wave number corresponding to the mixture with  $\sigma = 0.09$  Si/m is  $k_4 = (56.55 + i1.88) \text{ m}^{-1}$ , and that corresponding to  $\sigma = 4.2$  Si/m is  $k_4 = (82.61 + i60.22) \text{ m}^{-1}$ . In comparison, the wave number in air is  $k_2 = 6.28 \text{ m}^{-1}$ .

In order to drive the two coupled antennas in the zero-phase sequence, the applied voltages must be equal in magnitude and in phase, i.e.,  $V_1 = V_2$ .

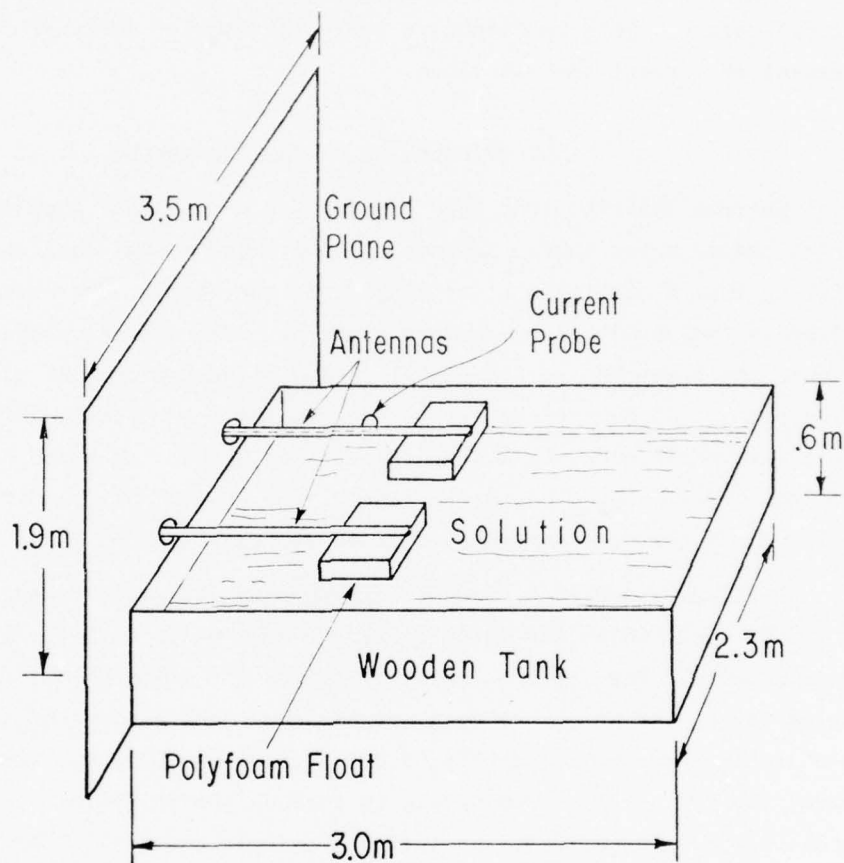


FIG. 5 SCHEMATIC DIAGRAM OF EXPERIMENTAL FACILITY

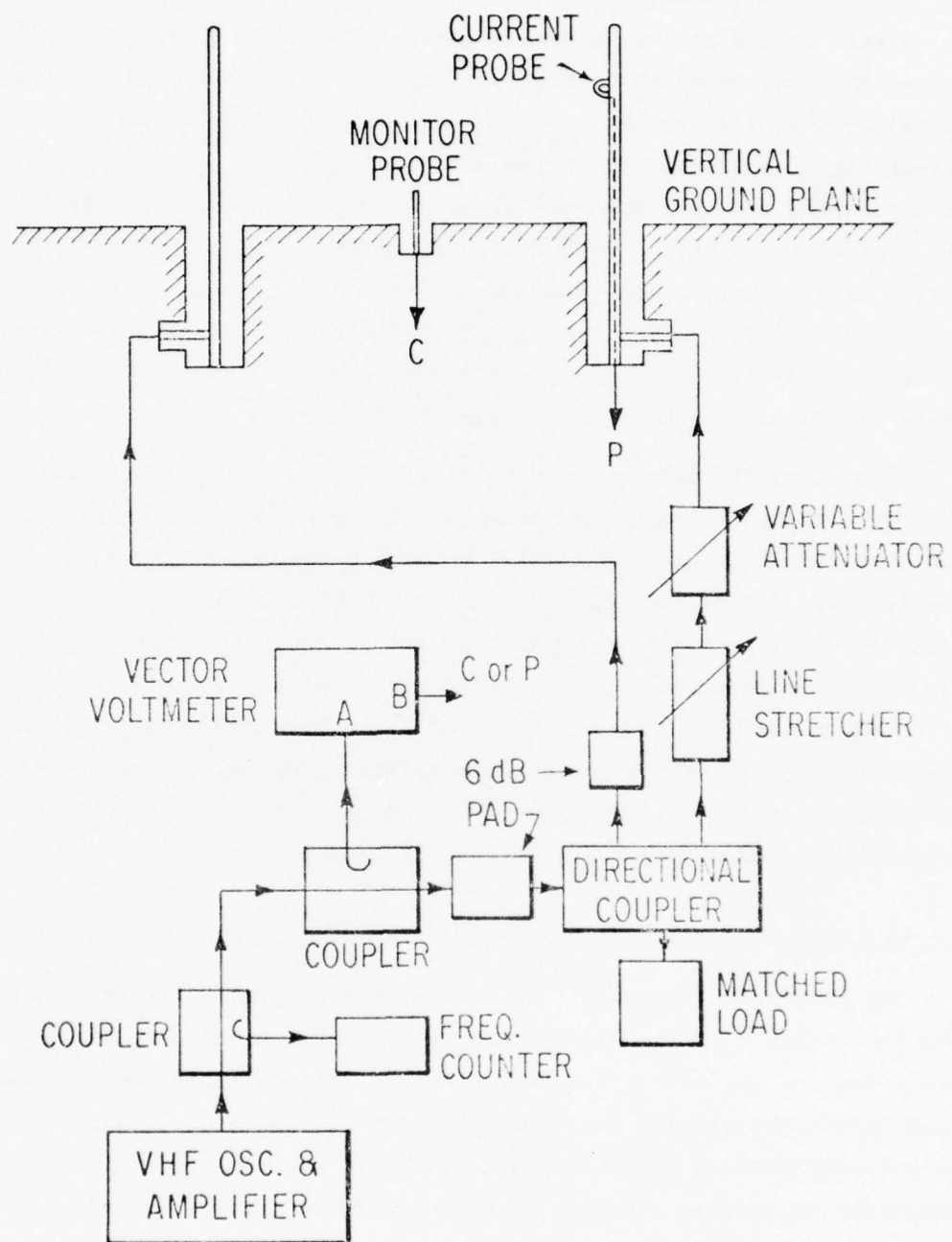


FIG.6 BLOCK DIAGRAM OF MEASURING CIRCUIT

For the first-phase sequence the two voltages must be equal in magnitude and  $180^\circ$  out of phase, i.e.,  $V_1 = -V_2$ . The adjustments for the first-phase sequence were made with the help of a monitor (monopole probe) midway between the two antennas as shown in Fig. 6. The relative amplitudes and phases of the voltages applied to the two antennas were varied until a null or deep minimum signal was observed in the output of the monitor. The adjustment for the zero-phase sequence involved first the adjustment for the first-phase sequence followed by the insertion of a 50 cm (i.e., a half-wavelength) long section of air line in the feed line of one of the antennas to shift its phase by  $180^\circ$ . The adjustment was checked with a small loop substituted for the monopole as the monitor. A null or deep minimum signal from the loop indicated that both antennas were driven in phase.

A total of 100 sets of current distributions were measured with a small loop moved along a slot in the antenna. The amplitude and phase of the current were recorded for each point. Typical measured distributions for two identical parallel antennas with open ends are shown by the successions of points in Fig. 7. For this particular set of data, the antennas were separated by the distance  $L = 0.3\lambda_2$  and were each at the height  $d = 0.0775\lambda_2$  above salt water with  $\sigma_4 = 4.2$  Si/m and  $\epsilon_{4r} = 81$ . The small circles in Fig. 7 are the measured points for the zero-phase sequence, the crosses for the first-phase sequence. Also shown in solid dots is the current distribution for infinite separation, i.e., for one antenna alone.

## 7. EVALUATION OF TERMINAL FUNCTIONS; COMPARISON OF THEORY AND EXPERIMENT

The theoretical formula (32) for current applies directly to a monopole when the factor 2 in the denominator is deleted. As already stated, all quantities for the currents in the antennas for the two phase sequences are known except the complex terminal functions  $\theta_s^{(m)}$ ,  $m = 0, 1$ , for which no analytically derived formulas are available. Accordingly, they have been determined to provide the best agreement between current distributions calculated from (32) and the corresponding measured ones of which those in Fig. 7 are an example. This is accomplished by normalizing the amplitude of the theoretical current to coincide with the experimental data at  $z = 0.25\lambda_2$  or  $z = 0.75\lambda_2$  - whichever yields better results - and then varying  $\theta_s^{(m)}$  (or, equivalently, the complex reflection coefficient  $\Gamma_s^{(m)}$ ) to establish a fit





between the theory and the experimental data in the sense of least-square errors. The details of this procedure are outlined in the Appendix. In effect, it yields measured values of  $r_s^{(m)}$  or  $\theta_s^{(m)}$  which can then be substituted in the theoretical formula. Typical distributions of current obtained in this manner are shown in Fig. 7 where the theoretical dotted curves have been matched to the measured points shown by small circles for the zero-phase sequence and the theoretical dashed curves have been matched to the measured points shown by crosses for the first-phase sequence. Both sets of curves are for distances between the antennas of  $L = 0.3\lambda_2$ . The solid line curves also shown in Fig. 7 have been fitted to the measured dots for the single antenna corresponding to infinite separation. All graphs in Fig. 7 apply to antenna heights of  $d = 0.0775\lambda_2$ . Similarly good agreement between the theoretical currents with measured  $\theta_s^{(m)}$  and measured currents have been obtained for other heights and distances between the coupled antennas. The results are summarized in the graphs of Figs. 8 and 9 which show the measured values of  $\theta_s^{(m)} = \rho_s^{(m)} - i\phi_s^{(m)}$  as a function of  $L/\lambda_2$  for coupled antennas with open ends over lake and sea water. When these values are substituted in (32), theoretical currents in good agreement with measured values are obtained for antennas over water with conductivities of 0.09 Si/m and 4.2 Si/m. The former is only slightly more conducting than many lakes, the latter corresponds to sea water.

A further check on the least-square determination of  $\theta_s^{(m)} = \rho_s^{(m)} - i\phi_s^{(m)}$ ,  $m = 0, 1$ , is obtained in its application to terminated antennas. With terminations consisting of a suitably chosen lumped resistor to obtain an optimum match in series with a quarter-wave extension of the horizontal-wire antenna, essentially traveling-wave distributions of current can be achieved with currents decreasing only slightly in amplitude over the entire length of the antenna from the driving point to the resistor and a linear change in phase. (An example is shown in Fig. 7 of [Sorbello et al., 1977].) Theoretically, a perfectly terminated antenna is characterized by  $\rho_s = \infty$ . With both  $Z_s = R_s - iX_s$  and  $Z_c = R_c(1 + i\phi_c)$  complex, the general formulas relating  $Z_s$  and  $Z_c$  with  $\rho_s$  and  $\phi_s$  are involved. They are given by [King, 1965]:

$$r_1 = \frac{R_s - \phi_c X_s}{R_c(1 + \phi_c^2)} = \frac{\sinh 2\rho_s}{\cosh 2\rho_s - \cos 2\phi_s} \quad (34)$$

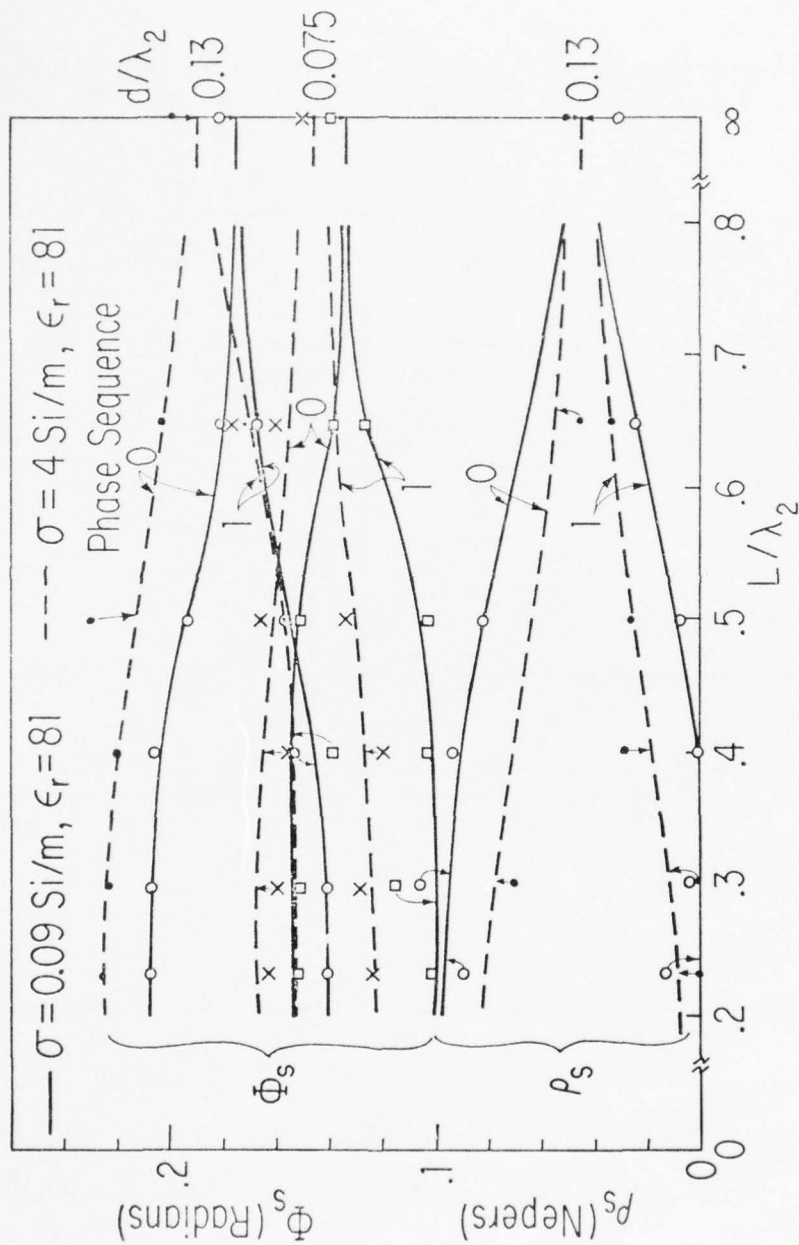


FIG. 8 PHASE AND ATTENUATION FUNCTIONS  $\Phi_s$  AND  $\rho_s$  CALCULATED FROM MEASURED CURRENTS WITH LEAST-SQUARES METHOD

• Phase Sequence 0  $\left\{ \frac{d}{\lambda_2} = 0.775 \right.$   $\times$  Phase Sequence 0  $\left\{ \frac{d}{\lambda_2} = 0.13 \right.$   
 ○ " " 1  $\left\{ \frac{d}{\lambda_2} = 0.775 \right.$  □ " " 1  $\left\{ \frac{d}{\lambda_2} = 0.13 \right.$   
 — Ideal Theory

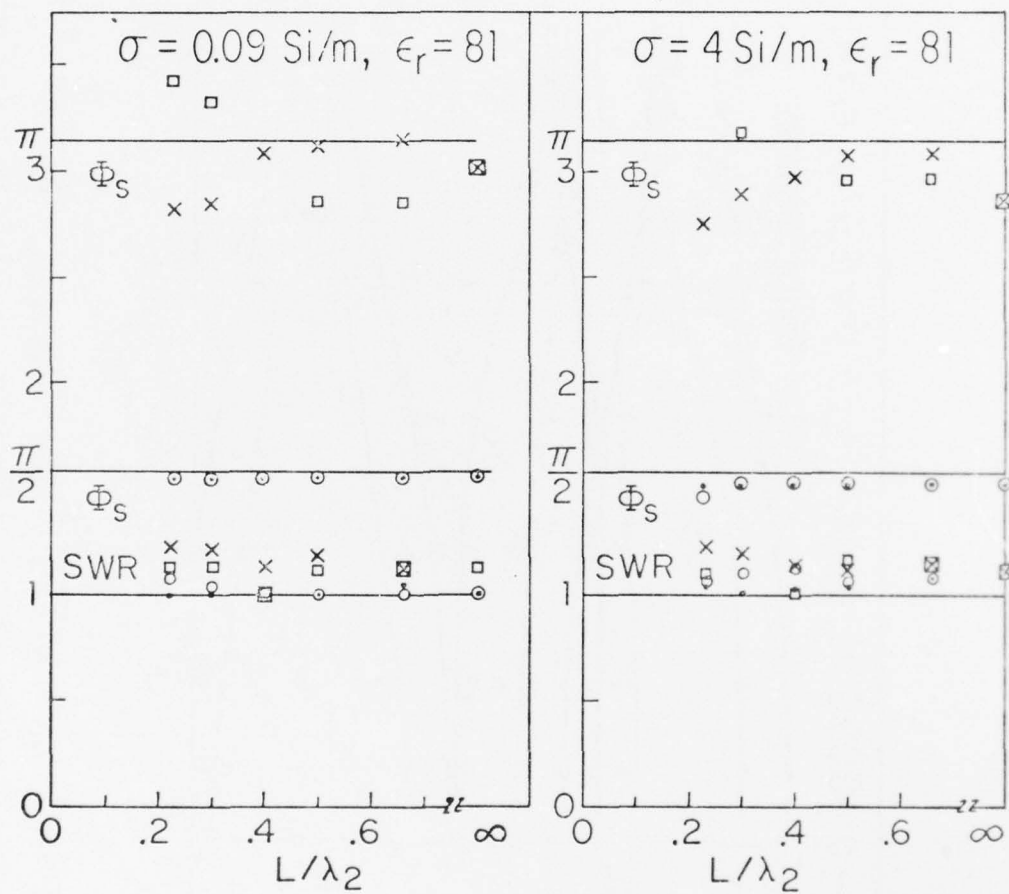


FIG. 9 PHASE CONSTANT  $\Phi_s$  AND  $\text{SWR} = \tanh^{-1} \rho_s$  CALCULATED FROM MEASURED CURRENTS BY LEAST SQUARES

$$x_1 = \frac{X_s + \phi_c R_s}{R_c (1 + \phi_c^2)} = \frac{-\sin 2\phi_s}{\cosh 2\rho_s - \cos 2\phi_s} \quad (35)$$

For the case at hand involving coupled antennas with region 2 air, (14) gives for the phase-sequence characteristic impedance

$$\begin{aligned} Z_c^{(m)} &= (\zeta_0 \beta_{LN}^{(m)} / 2\pi) [\ln(2d/a) + (-1)^m (1/2) \ln(1 + 4d^2/L^2)] [1 + i\alpha_{LN}^{(m)} / \beta_{LN}^{(m)}] \\ &= R_c^{(m)} (1 + i\phi_c^{(m)}) \quad , \quad m = 0, 1 \end{aligned} \quad (36)$$

where  $\zeta_0 \triangleq 120\pi$  ohms.  $\beta_{LN}^{(m)} = \beta_L^{(m)} / k_2$  and  $\alpha_{LN}^{(m)} = \alpha_L^{(m)} / k_2$ ,  $m = 0, 1$ , are given in Figs. 3 and 4 for lake and sea water. It is seen that  $\phi_c^{(m)} = \alpha_{LN}^{(m)} / \beta_{LN}^{(m)} \ll 1$  so that  $Z_c^{(m)} \triangleq R_c^{(m)}$ .

For a predominantly resistive termination in either phase sequence with  $R_s \gg |X_s|$ , (34) and (35) reduce to  $r_1 \triangleq R_s / R_c$ ,  $x_1 \triangleq X_s / R_c \triangleq 0$ . It follows from (35) that  $\phi_s \triangleq \pi/2$  or  $\pi$  and (35) reduces to  $r_1 = \tanh \rho_s$ ,  $\phi_s = \pi/2$ ;  $r_1 = \coth \rho_s$ ,  $\phi_s = \pi$ . Hence, as  $\rho_s \rightarrow \infty$  and  $r_1 \rightarrow 1$  from below,  $\phi_s = \pi/2$ ; as  $\rho_s \rightarrow \infty$  and  $r_1 \rightarrow 1$  from above,  $\phi_s = \pi$ . The mathematical limiting value of  $\phi_s$  when  $\rho_s = \infty$  is  $3\pi/4$ .

Since  $\rho_s \triangleq \tanh^{-1}(R_s/R_c)$ ,  $R_s < R_c$ , and  $\rho_s \triangleq \coth^{-1}(R_s/R_c)$ ,  $R_s > R_c$ ,  $\rho_s$  increases very steeply as  $R_s$  approaches  $R_c$ . Hence, a more convenient quantity for comparison with measurement is the standing-wave ratio which is defined by

$$\text{SWR} = \coth \rho_s \triangleq \begin{cases} R_s/R_c \geq 1, \phi_s = \pi \\ R_c/R_s \geq 1, \phi_s = \pi/2 \end{cases} \quad (37)$$

When  $\rho_s$  is large, the SWR is close to unity. In Fig. 8 are shown ideal theoretical graphs of  $\phi_s = \pi$  and  $\pi/2$  with  $\rho_s = \infty$  or  $\text{SWR} = 1$ . With them are plotted the measured values of  $\phi_s$  and the SWR as obtained from  $\rho_s$  for both lake and sea water with  $d/\lambda_2 = 0.0775$  and  $0.13$ . It is seen that the condition of match is very well confirmed. Note that for the height  $d/\lambda_2 = 0.13$ ,  $R_s > R_c$  so that  $\phi_s \triangleq \pi$ ; on the other hand, for  $d/\lambda_2 = 0.0775$ ,  $R_s < R_c$  so that  $\phi_s \triangleq \pi/2$ . These results indicate that the terminations were predominantly resistive and well selected to obtain traveling-wave distributions of current.



## 8. CONCLUSION

The theory of the horizontal-wire antenna over an electrically dense half-space is extended to parallel coupled antennas. The distributions of current have the simple transmission-line form with different complex wave numbers and characteristic impedances for the symmetrically and antisymmetrically driven antennas. Currents with arbitrary driving voltages can be obtained by superposition.

The simple transmission-line form for the currents in coupled horizontal-wire antennas with open ends in air over a dissipative or dielectric half-space is generalized by the addition of a terminating impedance  $Z_s$  that takes approximate account of radiation into the air and simultaneously provides the capacitive end-correction at the open end. The terminating impedance, expressed in terms of the terminal function  $\theta_s = \rho_s - i\phi_s$ , is determined by fitting measured currents to the theoretical ones. In addition to evaluating the terminal functions, the form of the theory is confirmed by the good agreement between theoretical and measured currents for open-ended antennas and the good agreement between theory and experiment in the terminal functions for traveling-wave antennas.

## 9. APPENDIX

In this Appendix the application of the least-square-error method is described.

Let  $z_n$  denote the position of the probe with reference to the driving point and  $A_n$  denote the amplitude of the current measured at  $z_n$ . The theoretical current is given by

$$I(z) = I_0 (e^{i\beta_L z} e^{-\alpha_L z} - R e^{-i\beta_L z} e^{\alpha_L z}) \quad (A1)$$

where  $R = \Gamma_s e^{i2k_L h}$  and  $\beta_L + i\alpha_L = k_L$ ;  $\Gamma_s$  is the complex reflection coefficient at  $z = h$ . The value of  $k_L$  is known theoretically. The absolute value of  $I(z)$  is

$$|I(z)| = |I_0| e^{-\alpha_L z} |1 - R e^{-i2\beta_L z} e^{2\alpha_L z}| \quad (A2)$$

Matching  $|I(z)|$  with  $A_n$  at  $n = n_0$  where  $z = z_0$  gives

$$|I_0| e^{-\alpha_L z_0} |1 - R e^{-i2\beta_L z_0} e^{2\alpha_L z_0}| = A_{n_0} \quad (A3)$$

Thus,

$$|I_0| = e^{\alpha_L z_0} A_{n_0} |1 - R e^{-i2\beta_L z_0} e^{2\alpha_L z_0}|^{-1} \quad (A4)$$

or

$$|I(z)| = \frac{e^{\alpha_L(z_0 - z)} |1 - R e^{-i2\beta_L z} e^{2\alpha_L z}|}{|1 - R e^{-i2\beta_L z_0} e^{2\alpha_L z_0}|} A_{n_0} \quad (A5)$$

The mean-square-error between the theory and the experimental data is

$$E = \frac{1}{N} \sum_{n=1}^N (|I(z_n)| - A_n)^2 \quad (A6)$$

where  $|I(z_n)|$  is given by (A5). By varying  $|R|$  from 0 to  $e^{-2\alpha_L h}$  and the phase

$\psi$  of  $R$  from 0 to  $2\pi$ , the value of  $R$  corresponding to the minimum mean-square-error is obtained. The complex terminal function  $\theta_s$  is calculated from  $R$  using the following equation:

$$\theta_s = -[(1/2)\ln R - ik_L h] = -(1/2)\ln \Gamma_s \quad (A7)$$

#### 10. REFERENCES

- King, R. W. P. (1956), Theory of Linear Antennas, 944 pp., Harvard University Press, Cambridge, Mass.
- King, R. W. P. (1965), Transmission-Line Theory, p. 102, Dover Publications, New York.
- King, R. W. P., T. T. Wu, and L. C. Shen (1974), The horizontal-wire antenna over a conducting or dielectric half-space: Current and admittance, Radio Sci., 9(7), 701-709.
- Sorbello, R. M. (1976), Eversion-Wave Antennas, Ph.D. Thesis, Harvard University, Cambridge, Mass.
- Sorbello, R. M., R. W. P. King, K.-M. Lee, L. C. Shen, and T. T. Wu (1977), The horizontal-wire antenna over a dissipative half-space: Generalized formula and measurements, submitted for publication.
- Wait, J. R. (1975), Theory of EM wave propagation through tunnels, Radio Sci., 10(7), 753-759.
- Wu, T. T., L. C. Shen, and R. W. P. King (1975), The dipole antenna with eccentric coating in a relatively dense medium, IEEE Trans. Antennas Propagat., AP-23(1), 57-62.

## B. Measured Currents on Two Coupled Collinear Beverage Antennas

Two Beverage antennas were arranged in a collinear configuration as shown in Fig. 1. The monopole was 1.0 m long to the terminating resistor and extended a quarter wavelength beyond this. The collinear, asymmetrical dipole was terminated with a resistor a quarter wavelength from each end. The forward arm of the dipole was one meter long to the resistor and extended beyond it a quarter wavelength; the backward arm consisted of the resistor and a section beyond it a quarter wavelength long. The height  $d$  of the antennas above the surface of the water was fixed at either 13 cm or 2.5 cm. The three resistors used to terminate the antennas were each  $330\ \Omega$  for  $d = 13$  cm and each  $220\ \Omega$  for  $d = 2.5$  cm. The separation  $g$  between the adjacent ends of the antennas was set at approximately either 1.5 cm or 18 cm. The conductivity of the solution was measured to be  $0.09\ \text{Si/m}$  for the first set of measurements, and was later changed to  $4.2\ \text{Si/m}$  for a second set.

Since the input impedance of the terminated monopole is approximately half that of the terminated asymmetrical dipole, it was necessary to introduce a 6 dB attenuator into the feedline of the monopole in order to maintain the same current amplitudes in the two collinear antennas. A phase shifter was used to adjust the relative phases of the two driving voltages. A symmetrical excitation with both antennas driven in phase with currents of equal amplitude was obtained with a 50 cm air-filled coaxial line inserted in one of the feedlines. Removal of this 50 cm line yielded antisymmetrical excitation with the two currents equal in amplitude but  $180^\circ$  out of phase.

The feedline for the dipole was completely submerged in the water tank to reduce interference with the antennas. Because of the attenuation experienced by fields in the water solution, no detectable change in the current distributions could be observed when the submerged cable was moved from one position to another.

Results of the measurements are summarized in Tables 1 through 5. It is seen that a coupling effect is in general negligible. The greatest effect was observed when the antennas were quite high above the lossy medium ( $d \approx$

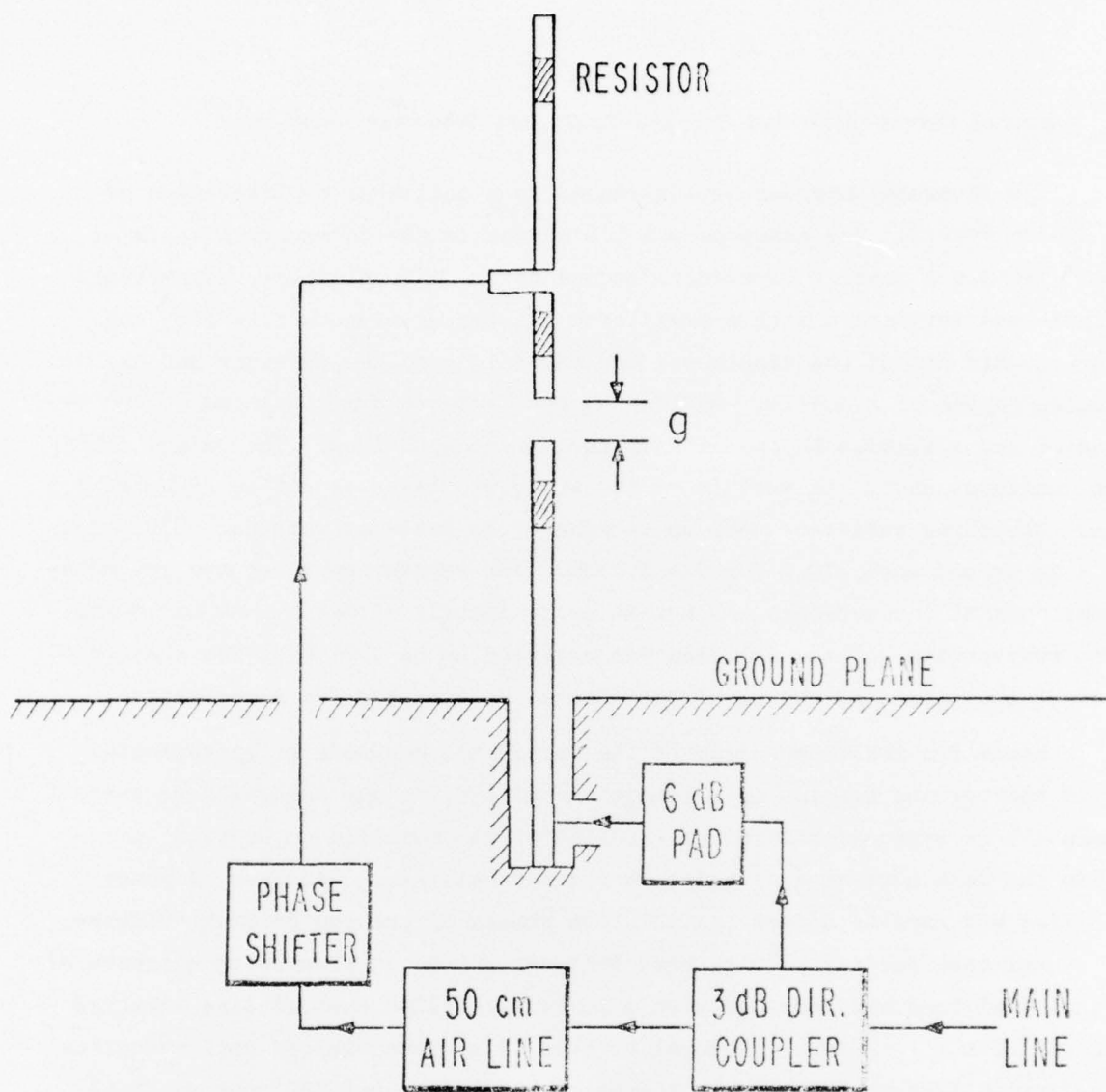


FIG. 1. COLLINEAR BEVERAGE ANTENNAS



$0.18\lambda_0$ ) with their adjacent ends separated from each other by a small gap ( $g \approx 0.02\lambda_0$ ) and when the medium had high conductivity ( $\sigma = 4.2 \text{ Si/m}$ ). Even in this case (Table 4) the mutual interaction caused a change of no more than  $10^\circ$  in the phase and no more than 1 dB in the amplitude of the current at a few points along the antenna as compared to the current on a single, isolated Beverage antenna. The coupling decreased as the gap  $g$  was increased, as the height  $d$  was decreased, and as the conductivity  $\sigma$  of the water was reduced.

In general, the currents on driven Beverage antennas in the collinear position are largely independent and like those on the same element when isolated.

TABLE 1

CURRENT ON MONOPOLE IN COLLINEAR ARRAY OF TWO BEVERAGE ANTENNAS

(Amplitude/Phase)

 $d = 2.5 \text{ cm}$  ,  $g = 1.2 \text{ cm}$  ,  $\sigma = 0.09 \text{ Si/m}$ 

z	Symmetrical Excitation	Single Monopole	Anti-Symmetrical Excitation
.10	5.5/38°	5.5/37°	5.6/39°
.15	5.5/18°	5.7/16°	5.6/20°
.20	5.5/-1°	5.5/-3°	5.5/1°
.25	5.5/-19°	5.5/-21°	5.5/-16°
.30	5.4/-36°	5.5/-39°	5.3/-33°
.35	5.2/-52°	5.3/-58°	5.1/-51°
.40	4.9/-71°	5.0/-74°	4.8/-70°
.45	4.6/-91°	4.7/-94°	4.5/-90°
.50	4.4/-112°	4.5/-117°	4.3/-111°
.55	4.3/-133°	4.5/-137°	4.3/-131°
.60	4.3/-153°	4.5/-157°	4.3/-151°
.65	4.4/-172°	4.6/-174°	4.3/-169°
.70	4.4/172°	4.7/170°	4.3/174°
.75	4.4/157°	4.6/155°	4.3/158°
.80	4.2/140°	4.3/139°	4.0/142°
.85	3.9/123°	3.8/121°	3.7/123°
.90	3.7/104°	3.6/103°	3.5/103°

TABLE 2

CURRENT ON MONOPOLE IN COLLINEAR ARRAY OF TWO BEVERAGE ANTENNAS

(Amplitude/Phase)

 $d = 13 \text{ cm}$  ,  $g = 1.5 \text{ cm}$  ,  $\sigma = 0.09 \text{ Si/m}$ 

z	Symmetrical Excitation	Single Monopole	Anti-Symmetrical Excitation
.10	5.1/29°	5.5/33°	5.7/37°
.15	5.4/6.5°	5.5/13°	5.7/18°
.20	5.6/-13°	5.5/-6°	5.5/0°
.25	5.9/-29°	5.6/-22°	5.5/-18°
.30	6.0/-44°	5.5/-39°	5.3/-36°
.35	6.0/-58°	5.3/-57°	5.1/-55°
.40	5.5/-74°	5.1/-75°	5.0/-75°
.45	5.1/-92°	4.9/-95°	5.0/-95°
.50	4.6/-113°	4.8/-116°	4.9/-116°
.55	4.6/-135°	4.9/-135°	5.2/-134°
.60	4.6/-158°	5.0/-155°	5.2/-151°
.65	4.9/-178°	5.1/-172°	5.3/-167°
.70	5.2/165°	5.3/172°	5.2/178°
.75	5.5/151°	5.3/156°	5.2/162°
.80	5.5/137°	5.1/140°	4.9/144°
.85	5.3/123°	4.9/122°	4.6/127°
.90	5.0/107°	4.7/104°	4.4/106°

TABLE 3

CURRENT ON MONOPOLE IN COLLINEAR ARRAY OF TWO BEVERAGE ANTENNAS

(Amplitude/Phase)

 $d = 13 \text{ cm}$  ,  $g = 18 \text{ cm}$  ,  $\sigma = 0.09 \text{ S/m}$ 

$z$	Symmetrical Excitation	Single Monopole	Anti-Symmetrical Excitation
.10	5.4/34°	5.5/33°	5.5/34°
.15	5.5/13°	5.5/13°	5.5/14°
.20	5.4/-7°	5.5/-6°	5.6/-5°
.25	5.6/-24°	5.6/-22°	5.6/-22°
.30	5.6/-41°	5.5/-39°	5.5/-39°
.35	5.5/-58°	5.3/-57°	5.4/-56°
.40	5.4/-75°	5.1/-75°	5.2/-74°
.45	5.2/-93°	4.9/-95°	5.0/-94°
.50	4.9/-113°	4.8/-116°	4.9/-115°
.55	5.0/-133°	4.9/-135°	5.1/-135°
.60	4.9/-152°	5.0/-155°	5.2/-154°
.65	5.0/-171°	5.1/-172°	5.3/-171°
.70	5.2/172°	5.3/172°	5.4/173°
.75	5.4/155°	5.3/156°	5.5/158°
.80	5.2/140°	5.1/140°	5.4/141°
.85	5.0/123°	4.9/122°	5.0/125°
.90	4.7/105°	4.7/104°	4.8/106°

TABLE 4

CURRENT ON MONOPOLE IN COLLINEAR ARRAY OF TWO BEVERAGE ANTENNAS  
(Amplitude/Phase)

$d = 13 \text{ cm}$  ,  $g = 1.0 \text{ cm}$  ,  $\sigma = 4.2 \text{ Si/m}$

$z$	Symmetrical Excitation	Single Monopole	Anti-Symmetrical Excitation
.10	6.6/7°	7.3/12°	7.6/15°
.15	6.9/-16°	7.5/-8°	7.6/-4°
.20	7.3/-36°	7.4/-26°	7.4/-21°
.25	7.8/-52°	7.4/-43°	7.2/-38°
.30	8.0/-67°	7.2/-61°	7.0/-57°
.35	7.9/-81°	7.1/-78°	6.8/-76°
.40	7.5/-96°	6.9/-97°	6.7/-97°
.45	6.9/-114°	6.7/-117°	6.7/-117°
.50	6.3/-134°	6.6/-137°	6.9/-136°
.55	6.2/-156°	6.8/-155°	7.3/-155°
.60	6.2/-179°	6.9/-174°	7.4/-171°
.65	6.5/160°	7.0/169°	7.3/172°
.70	6.9/143°	7.0/152°	7.2/158°
.75	7.4/128°	7.1/135°	7.1/141°
.80	7.3/113°	6.8/118°	6.6/123°
.85	7.0/98°	6.5/101°	6.2/103°
.90	6.6/82°	6.3/82°	6.0/81°



TABLE 5

CURRENT ON MONOPOLE IN COLLINEAR ARRAY OF TWO BEVERAGE ANTENNAS  
(Amplitude/Phase)

$d = 13 \text{ cm}$  ,  $g = 17 \text{ cm}$  ,  $\sigma = 4.2 \text{ Si/m}$

$z$	Symmetrical Excitation	Single Monopole	Anti-Symmetrical Excitation
.10	6.9/13°	7.3/12°	7.4/12°
.15	6.9/-11°	7.5/-8°	7.6/-9°
.20	6.9/-28°	7.4/-26°	7.6/-27°
.25	7.1/-46°	7.4/-43°	7.7/-44°
.30	7.1/-62°	7.2/-61°	7.6/-61°
.35	7.0/-80°	7.1/-78°	7.4/-79°
.40	6.8/-97°	6.9/-97°	7.1/-98°
.45	6.6/-115°	6.7/-117°	7.0/-118°
.50	6.3/-135°	6.6/-137°	7.0/-137°
.55	6.4/-155°	6.8/-155°	7.3/-157°
.60	6.4/-175°	6.9/-174°	7.4/-175°
.65	6.4/166°	7.0/169°	7.5/168°
.70	6.6/149°	7.0/152°	7.5/152°
.75	6.9/132°	7.1/135°	7.7/136°
.80	6.8/115°	6.8/118°	7.3/119°
.85	6.6/99°	6.5/101°	6.8/101°
.90	6.3/80°	6.3/82°	6.5/82°

#### IV. PUBLICATIONS

##### A. Scientific Reports

Scientific Report No. 1 (Vols. I and II): R. M. Sorbello, "The Beverage Wave Antenna: Currents, Charges and Admittances. I. Theoretical Analysis; Experimental Equipment and System Calibration. II. Experimental Measurements," RADC/ETER Contract F19628-76-C-0057, 1977.

Scientific Report No. 2: R. M. Sorbello, "The Beverage Wave Antenna: Radiation Field Patterns," RADC/ETER Contract F19628-76-C-0057, 1977.

Final Report: R. M. Sorbello, R. W. P. King, K.-M. Lee, L. C. Shen, and T. T. Wu, "Arrays of Beverage Antennas," RADC/ETER Contract F19628-76-C-0057, 1977.

##### B. Papers for Publication

L. C. Shen, R. W. P. King and R. M. Sorbello, "Measured Field of a Directional Antenna Submerged in a Lake," IEEE Trans. Antennas Propagat., AP-24, pp. 891-894, November 1976.

R. M. Sorbello, R. W. P. King, K.-M. Lee, L. C. Shen, and T. T. Wu, "The Horizontal-Wire Antenna Over a Dissipative Half-Space: Generalized Formula and Measurements," IEEE Trans. Antennas Propagat., accepted for publication.

L. C. Shen, K.-M. Lee, and R. W. P. King, "Coupled Horizontal-Wire Antennas Over a Conducting or Dielectric Half-Space," submitted for publication.

##### C. Papers Presented at Scientific Meetings

R. M. Sorbello, "Properties of the Horizontal-Wire Antenna Over an Imperfect Conductor with Special Application to the Beverage Wave Antenna," presented at the 1975 Annual URSI/USNC Meeting, Boulder, Colorado, October 1975.

R. M. Sorbello and R. W. P. King, "The Horizontal-Wire Antenna Over an Imperfect Conductor," presented at the 1976 Annual URSI/USNC Meeting, University of Mass., Amherst, October 1976.

##### D. Related Papers

R. W. P. King, T. T. Wu, and L. C. Shen, "The Horizontal-Wire Antenna Over a Conducting or Dielectric Half-Space: Current and Admittance," Radio Sci., 9, pp. 701-709, July 1974.

T. T. Wu, L. C. Shen, and R. W. P. King, "The Dipole Antenna with Eccentric Coating in a Relatively Dense Medium," IEEE Trans. Antennas Propagat., AP-23, pp. 57-62, January 1975.

K.-M. Lee and R. W. P. King, "The Terminated Insulated Antenna," Radio Sci., 11, pp. 367-373, April 1976.

K.-M. Lee, T. T. Wu, and R. W. P. King, "Theory of Insulated Linear Antenna in a Dissipative Medium," Radio Sci., scheduled to appear in March/April 1977 issue.



# *MISSION of Rome Air Development Center*

RADC plans and conducts research, exploratory and advanced development programs in command, control, and communications (C<sup>3</sup>) activities, and in the C<sup>3</sup> areas of information sciences and intelligence. The principal technical mission areas are communications, electromagnetic guidance and control, surveillance of ground and aerospace objects, intelligence data collection and handling, information system technology, ionospheric propagation, solid state sciences, microwave physics and electronic reliability, maintainability and compatibility.

Printed by  
United States Air Force  
Hanscom AFB, Mass. 01731